We are IntechOpen, the world's leading publisher of Open Access books Built by scientists, for scientists

4,800
Open access books available

122,000
International authors and editors

135M
Downloads

Our authors are among the

154
Countries delivered to

TOP 1%
most cited scientists

12.2%
Contributors from top 500 universities

WEB OF SCIENCE™

Selection of our books indexed in the Book Citation Index in Web of Science™ Core Collection (BKCI)

Interested in publishing with us?
Contact book.department@intechopen.com

Numbers displayed above are based on latest data collected.
For more information visit www.intechopen.com

23

Optical Fibers and Optical Fiber Sensors Used in Radiation Monitoring

Dan Sporea[1], Adelina Sporea[1],
Sinead O'Keeffe[2], Denis McCarthy[2] and Elfed Lewis[2]
[1]*National Institute for Laser, Plasma and Radiation Physics, Laser Metrology Laboratory,*
[2]*Optical Fibre Sensors Research Centre, University of Limerick*
[1]*Romania,*
[2]*Ireland*

1. Introduction

By their very nature, optical fibers and, by extension, intrinsic and extrinsic optical fiber-based sensors are promising devices to be used in very different and complex environments considering their characteristics such as: capabilities to work under strong electromagnetic fields; possibility to carry multiplexed signals (time, wavelength multiplexing); small size and low mass; ability to handle multi-parameter measurements in distributed configuration; possibility to monitor sites far away from the controller; their availability to be incorporated into the monitored structure; wide bandwidth for communication applications. In the case of the optical fibers, the possibility to be incorporated into various types of sensors and actuators, free of additional hazards (i.e. fire, explosion), made them promising candidates to operate in special or adverse conditions as those required by space or terrestrial applications (spacecraft on board instrumentation, nuclear facilities, future fusion installations, medical treatment and diagnostics premises, medical equipment sterilization). Major advantages to be considered in using optical fibers/optical fiber sensors for radiation detection and monitoring refer to: real-time interrogation capabilities, possibility to design spatially resolved solutions (the capability to build array detectors), in-vivo investigations (i.e. inside the body measurements).

As information on the behavior and operation of optical fibers/optical fiber sensors under irradiation conditions are scattered over a great variety of journal papers and conference contributions dealing with many different fields (nuclear science and engineering; measurement science; material science; radioprotection; nuclear medicine and radiology; sensor design; radiation dosimetry; fusion installations concepts; particle accelerators; astrophysics and space science; defense and security; lasers, optics, optical fibers and optoelectronics; physics and applied physics; scientific instrumentation; radiation effects) we decided to design this book chapter as a comprehensive review on the subject. The chapter opens with some general considerations on the radiation–matter interaction, and continues with a review of irradiation effects on different types of optical fibers (silica optical fibers, plastic optical fibers, special optical fibers), effects which can be considered when radiation sensors are developed. The next issue addressed refers to environments where optical fibers/optical fiber sensors are employed for radiation monitoring/

dosimetry. The main part of the chapter is dedicated to the presentation of major proposed designs for intrinsic and extrinsic optical fiber sensors for radiation measurements. The experimental set-ups and irradiation conditions we used for the assessment of irradiation effects on various optical fibers are introduced and samples from our results illustrate the possible use of such optical fibers in radiation monitoring/dosimetry. The Romanian team focused its work on tests of silica and sapphire optical fibers subjected to different irradiation conditions (alpha particles, beta, gamma and X rays, neutron), while the Limerick group investigated radiation detectors based on plastic optical fibers, under gamma and X-rays irradiation.

Radiation induced effects in materials and devices are evaluated based on the energy losses resulting upon the interaction between highly energetic radiation and matter (Wrobel, 2005). Losses associated to these interactions can imply atoms ionization or can induce non-ionizing effects, such as changes of the vibrational/rotational states of molecules, atoms vibrations or atoms displacement. Generically, the term highly energetic radiation covers: a) uncharged particles – photons (gamma-rays, X-rays); b) charged light (electrons, positrons) and heavy (different types of ions) particles; c) nucleus constituents (neutrons, protons). Accelerated alpha particles (two protons and two neutrons bounded) or electrons, as well as high energy neutrons or photons can produce an atom's ionization. Depending on their energy, charge particles and nucleons can lead to either elastic or non-elastic interactions. On the other hand, lower energy photons can contribute to phenomena such as Rayleigh scattering (elastic scattering of photons by atoms or molecules), Compton scattering (the decrease of a X-ray or gamma-ray energy as it undergoes a non-elastic interaction with matter, the lost energy being transferred to a scattering electron as part of a ionizing process), photo-electric effect (the emission of electrons by a solid, liquid or gas upon the absorption of photons in that material) or pair production (the generation of an electron-positron pair as photons, having sufficient energy, interact with a nucleus). The occurrence of a particular phenomenon depends on the energy spectrum of the incident photons and the interaction cross sections (depending on the material involved). Light charged particles (i.e. electrons) when travelling inside a material are deflected by the surrounding atoms and lose energy, which is converted to photon energy, so, a continuum spectrum electromagnetic radiation is generated (Bremsstrahlung or deceleration radiation). Cerenkov radiation (a continuum spectrum optical radiation having a higher intensity at the UV wavelength end of the optical spectral range) is produced when a charged particle (i.e. electron) propagates within a dielectric medium with a speed higher than the phase velocity of the light in that medium. The molecules of the medium are polarized by the travelling particles and, returning to the ground state, emit visible optical radiation.

2. Optical fibers performances under irradiation

Exposed to ionizing radiation, silica optical fibers exhibit effects such as: radiation induced absorption (RIA), radiation induced luminescence (RIL), increase of the optical radiation scattering as it propagates over the fiber length, thermoluminescence, change of the waveguide refractive index. RIA and RIL effects contribute, generally speaking, to the degradation of the signal-to-noise ratio of the signal transmitted over the optical fiber guide. Attempts were made to reformulate the problem and to use these effects as a measure of the dose rate/total dose of the radiation to which the optical fiber is exposed.

In assessing the behavior of silica optical fibers under irradiation one has to consider several premises which have a major influence on the irradiation induced absorption, and hence on a would-be application of such optical fibers to radiation dosimetry. The RIA is affected by:

1. the manufacturing conditions, the parameters related to the technology used in producing the optical fiber: the deposition conditions, the draw process characteristics – draw speed, fiber drawing tension, the preform deposition temperature, oxygen-to-reagent ratio (02/R) used during core and clad deposition (Friebele, 1991; Girard et al., 2006; Hanafusa et al., 1986);
2. the existence, prior to the irradiation, of some precursors (Miniscalco et al., 1986);
3. the dopants present in the optical fiber core or cladding (pure silica, or doped with Ce, Er, Ge, F, N, P, Yb, high-OH, low-OH, high-Cl, low-Cl, H2-loading), (Arvidsson et al., 2009; Berghmans, 2006; Berghmans et al., 2008; Bisutti et al., 2007; Brichard & Fernandez Fernandez, 2005; Friebele, 1991; Girard et al., 2004a; Girard et al., 2004b; Girard et al., 2008; Griscom et al., 1996; Henschel et al., 1992; Kuyt et al., 2006; Lu et al., 1999; Mady et al., 2010; Paul et al., 2009; Regnier et al., 2007; Vedda et al., 2004; Wijnands et al., 2007), in some situations such ingredients contribute to the radiation hardening (Brichard et al., 2004; Brichard & Fernandez Fernandez, 2005; Girard et al., 2009);
4. the residual substances remaining after the manufacturing process, as for example chlorine having an associated color center in the UV spectral range, which can extend into the visible (Girard et al., 2008; Girard & Marcandella, 2010);
5. the type of radiation to which the optical fiber is subjected (Arvidsson et al., 2009; Bisutti et al., 2007; Brichard et al., 2001; Calderón et al., 2006; Girard et al., 2004a; Girard et al., 2004b; Girard et al., 2006; Girard et al., 2008; Merlo & Cankoçak, 2006; Toh et al., 2004; Yaakob et al., 2011);
6. the irradiation conditions: total dose, dose-rate, steady-state, pulsed, cyclic (Arvidsson et al., 2009; Berghmans, 2006; Berghmans et al., 2008; Kuhnhenn, 2005; Lu et al., 1999; Paul et al., 2009 ; Thériault, 2006; Wijnands et al., 2007);
7. the annealing effect and the temperature stress applied to the optical fiber during or post irradiation (Okamoto et al., 2004; Thériault, 2006; Toh et al., 2004; Tsuchiya et al., 2011);
8. the optical spectral band considered for the RIA evaluation (Regnier et al., 2007);
9. the optical fiber coating (Brichard, 2002; Gusarov et al., 2008b);
10. the photobleaching process and the level of the optical power injected into the optical fiber for measurement and its wavelength (Arvidsson et al., 2009; Miniscalco et al., 1986; Thériault, 2006; Treadaway et al.,1975).

The complexity of changes induced by highly energetic radiation in the optical transmission of silica optical fibers is governed by the optical fiber design, i.e. core-cladding dopants and diameter ratio (Deparis et al., 1997; Friebele, 1991; Girard et al., 2004a; Girard et al., 2004b; Kuhnhenn, 2005; Paul et al., 2009), and by the multitude of color centers activated under the irradiation process, such as (Brichard & Fernandez Fernandez, 2005; Origlio, 2009):

1. Ge centers: GeE', Ge(1), Ge(2), GEC, GeX, Ge-NBOH (Non-Bridging Oxygen Hole) (Alessi et al., 2010 ; Bisutti et al., 2007; Girard et al., 2006 ; Girard et al., 2008; Lu et al., 1999; Wijnands et al., 2007) ;
2. P centers: P1, P2, P4, Phosphorus-Oxygen-Hole - POHC (Bisutti et al., 2007; Girard et al., 2006; Girard et al., 2011 ; Paul et al., 2009; Wijnands et al., 2007) ;
3. silica related paramagnetic centers (Non-Bridging Oxygen Hole - NBOHC, PerOxy-Radical - POR, SiE', Self-Trapped Hole - STH 1/2) or diamagnetic centres (Oxygen

Deficient Centre – ODC; Peroxy Linkage – POL), (Berghmans et al., 2008; Girard et al., 2008).

In order to distinguish the contribution of various color centers to the irradiation induced absorption in silica optical fibers, complementary investigations, apart from the off-line/on-line optical transmission measurements, were carried-out: Electron Paramagnetic Resonance – EPR (Girard et al., 2008; Radiation effects, 2007; Sporea et al., 2010a; Weeks & Sonder, 1963), luminescence (Girard et al., 2005; Girard et al., 2006; Sporea et al., 2010a; Miniscalco et al., 1986), thermoluminescence (Espinosa et al., 2006; Hashim et al., 2008; Mady et al., 2010; Sporea et al., 2010b; Yaakob et al., 2011), confocal microscopy luminescence and Raman analysis (Girard et al., 2008; Origlio, 2009), time resolved photoluminescence (Cannas et al., 2008). Based on the results derived from different sources, a decomposition of the optical absorption spectra by using Gaussian bands associated to known color centers can be performed (Girard et al., 2008; Girard et al., 2011; Sporea et al., 2010a).

Apart from the aspects previously described (increase of the optical absorption in irradiated optical fibers, post irradiation luminescence and thermoluminescence effects) other phenomena have to be considered as prospective candidates for the use of optical fibers in radiation monitoring:

1. generation of Cerenkov radiation when optical fibers are subjected to a charged particle flux;
2. radiation induced luminescence (RIL) in optical fibers under irradiation (Skuja et al., 1996).

Traveling in a dielectric, transparent media, a charged particle (i.e. electron), having a velocity greater than the optical radiation phase velocity in that medium, interact with medium molecules by polarizing them. As the molecules return very fast to their ground state an optical radiation is emitted (Cerenkov, 1958). The optical radiation has a continuum distribution over the UV-visible spectral range.

As the emitted radiation spectrum varies with $1/\lambda^3$, the spectrum of the Cerenkov radiation is predominantly in UV-blue. Investigations on the generation of Cerenkov radiation were carried out for both silica and plastic optical fibers, such as polymethylmethacrylate - PMMA (Intermite et al., 2009; Jang et al., 2010a). The efficiency of coupling to and detecting the Cerenkov radiation with an optical fiber is a function of the type of optical fiber (its refractive index), the particles energy, the irradiation geometry: angle of incidence of the particle beam on the optical fiber axis, the optical fiber NA, the distance between the particle trajectory and the optical fiber axis (Goettmann et al., 2005; Jang et al., 2010a; Jang et al., 2011a).

In the case of a PMMA fiber with n = 1.49, for an electron beam energy of 6 MeV the maximum value for θ is 47.7^0 (Jang et al., 2010a), while for a silica optical fiber (n = 1.46) and a energy of the electron beam of 175 keV the Cerenkov radiation angle was evaluated to be about 46^0 (Intermite et al., 2009).

Gamma-rays can lead to the generation of Cerenkov radiation only if a Compton converter target is placed between the gamma source and the optical fiber. Photons incident on the converter produce electrons through the Compton Effect, with electrons further used to generate Cerenkov radiation. The efficiency of the conversion from gamma-ray to optical radiation depends on (Pruett et al., 1984): the target material (the best one proved to be beryllium), its thickness, the distance between the target and the optical fiber, the type of optical fiber, the angle between the gamma-ray trajectory (as a collimating scheme was

employed) and the optical fiber axis, the energy of the gamma-ray (investigations were done with a ^{60}Co source - the 1.17 and 1.33 MeV lines, and a ^{24}Na with its 1.38 and 2.76 MeV lines).

Optical materials, as per se or included in optical fibers, exhibit radioluminescence (radiation induced luminescence – RIL): visible radiation is emitted as long as the materials are exposed to ionizing ration. This signal is generally superposed over the Cerenkov spectrum, but can be distinguished by its narrow band emission spectra. The radioluminescent peaks observed, function of the material investigated, its dopants and the type of the irradiation, are located from UV - 185 nm, 250 nm, 285 nm, to visible - 420 nm, 450 nm, 696 nm (Toh et al., 2002; Treadaway et al., 1975; Yoshida et al., 2007). The superposition of the two spectra makes the discrimination of the luminescence signal difficult, and so, several methods to improve the S/N in detecting the radioluminescent signal against the Cerenkov radiation were developed: the gated detection of the luminescence (Justus, 2006; Plazas, 2005), different time frames or the different angular distribution of the two signals are used to detect the RIL (Akchurin et al., 2005); the subtraction method by employing a dummy optical fiber to record the Cerenkov radiation separately; an optical filter or a set-up based on a spectrometer (Archambault, 2005; Lee et al., 2007b; Jang et al., 2010a; Jang et al., 2011a).

An alternative to the generation of radioluminescence in optical materials is represented by the use of commercially available scintillating optical fibers as those delivered by Saint-Gobain Crystals and Detectors – France (Saint-Gobain, 2005) - core material: Polystyrene, core refractive index: 1.6, cladding material: acrylic, cladding refractive index: 1.49, NA: 0.58, scintillation efficiency: 2.4%, trapping efficiency: 3.4%, by Kuraray Co. (Japan) or specially designed ones, as Ce doped optical fibers (Chiodini et al., 2009).

Additional effects produced in silica optical fibers under irradiation refer to:

1. the change of the silica density observed either during gamma irradiation tests on distributed optical fiber sensors based on Brillouin scattering: a non-linear increase with the total dose of the measured frequency and Brillouin FWHM line width (Alasia et al., 2006), or under soft X-ray or reactor irradiation (Primak et al., 1964);
2. the modification of the refractive index of silica subjected to gamma-ray (Fernandez Fernandez et al., 2003).

In concluding this section on silica optical fibers, it is worth mentioning the behaviour of fiber Bragg gratings (FBGs) manufactured in silica optical fibers as they are exposed to irradiation, considering some authors suggestion to use such sensors as radiation detectors (Krebber et al., 2006). Several tests were run to evaluate the FBGs radiation hardness under neutron and gamma-ray exposure, in order to assess their possible use for temperature or stress monitoring in nuclear environments. Various types of FBGs as it concerns the optical fiber material, and the fabrication technology were used: Ge-doped (10 mol % GeO_2, Accutether AT120) with and without H_2 or D_2 loading (Gusarov et al., 2002; Gusarov et al., 2008a), B/Ge co-doped photo sensitive fiber (Maier, 2005), low-P content and N-doped optical fibers (Gusarov et al., 1999a), grating written by classical UV methods or using fs UV laser radiation (Gusarov et al., 2010). Gamma-ray pre-irradiation treatment or UV exposure of the sample before the nuclear reactor in core irradiation was also carried out in order to increase the immunity to irradiation effects (Fernandez Fernandez et al., 2001; Gusarov et al., 2008a). The Bragg gratings were investigated either in transmission or reflection, the parameters tested under irradiation were: the grating peak wavelength shift, the device

transmission/reflectivity, the Full-Width Half-Maximum (FWHM), the temperature sensitivity of the device. Studies revealed that the FBGs coating can play an important role in the radiation sensitivity of the sensor (Gusarov et al., 2008). Generally, under gamma irradiation, the FWHM parameter was not affected by the irradiation, while a shift of the peak wavelength was noticed, as being dependent of the total irradiation dose and the dose rate - the wavelength shift is directed towards longer (Caponero et al., 2007; Fernandez Fernandez et al., 2002; Maier et al., 2005a) or shorter wavelengths (Maier et al., 2005), accompanied by a saturating effect and the decrease of the device reflectivity. Depending on the fabrication process and on the optical fiber composition, highly doped Ge optical fibers proved to be less sensitive to gamma irradiation, while hydrogen loaded optical fibers show a higher sensitivity (Gusarov et al., 1999; Gusarov et al., 2002). In some situations, under mixed gamma-neutron irradiation, the FWHM of the FBGs had also increased, suggesting the partial erasing of the written grating (Fernandez Fernandez et al., 2001). The temperature coefficient of the FBG is not affected by gamma irradiation (Gusarov et al., 1999b).

Investigations into the radiation degradation of Poly(methyl methacrylate) (PMMA) (Yoshida & Ichikawa, 1995) show that the effects of ionizing radiation can be divided into two sections, namely main-chain scission (degradation) and crosslinking. In many polymers both processes take place in parallel with one another, however in certain cases the scission predominates the crosslinking, and such polymers are known as degrading polymers. PMMA, shown in Fig. 1, is one such polymer.

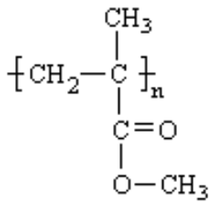

Fig. 1. PMMA polymer molecule.

Yoshida and Ichiwkawa (Yoshida & Ichikawa, 1995) report that the side-chain is initially affected by the gamma irradiation and the radical formed is a precursor for the main chain scission. When PMMA is irradiated with ionizing radiation, such as gamma radiation, a free radical is generated on the ester side-chain, $-\mathrm{COO\dot{C}H_2}$.

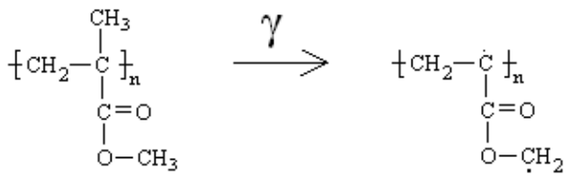

(1)

This side chain radical may be generated in a number of ways (Ichikawa, 1995), by direct action of ionizing radiation:

$$-\mathrm{COOCH_3} + \gamma \rightarrow -\mathrm{COO\dot{C}H_2} + \mathrm{H} \tag{2}$$

by proton transfer of the side-chain cation:

$$\begin{aligned} -\mathrm{COOCH_3} + \gamma &\rightarrow -\mathrm{COOCH_3^+} + \mathrm{e^-} \\ -\mathrm{COOCH_3^+} &\rightarrow -\mathrm{COO\dot{C}H_2} + \mathrm{H^+} \end{aligned} \tag{3}$$

or by hydrogen abstraction:

$$-\mathrm{COOCH_3} + \mathrm{H} \rightarrow -\mathrm{COO\dot{C}H_2} + \mathrm{H_2} \tag{4}$$

The side-chain radical remains stable at temperatures below 200 K. Above 210 K, the side-chain radical coverts to a scission type radical due to the detachment of the side chain. This is followed by the β-scission of the main-chain radical and is shown in equations 5 and 6.

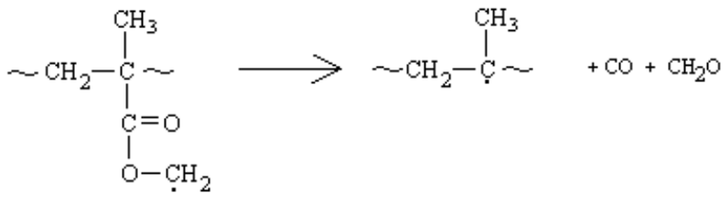

(5)

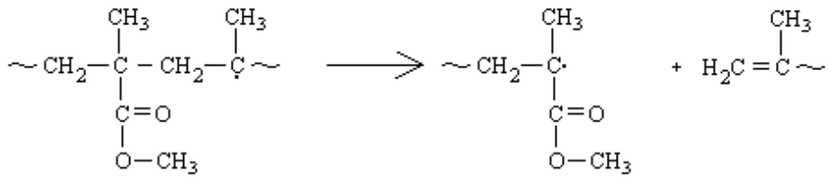

(6)

The Beer-Lambert law can be used to determine the radiation dose absorbed. The absorption co-efficient, α, is given by equation 7 (O'Keeffe et al, 2007).

$$\alpha = -\frac{1}{\mathrm{L_0}} \log \left\{ \frac{\mathrm{P}(\lambda)}{\mathrm{P^0}(\lambda)} \right\}, \tag{7}$$

where $\frac{\mathrm{P}(\lambda)}{\mathrm{P^0}(\lambda)}$ is the ratio of the spectral radiant power of light transmitted through the irradiated dosimeter to that of the light transmitted in the absence of the dosimeter.

The Beer-Lambert law is used to determine the radiation-induced attenuation. The radiation-induced attenuation is given by equation 8.

$$\mathrm{RIA(dB)} = -\frac{10}{\mathrm{L_0}} \log \left\{ \frac{\mathrm{P_T}(\lambda, \mathrm{t})}{\mathrm{P_T^0}(\lambda)} \right\}, \tag{8}$$

here L_0 is the irradiated length of fiber, $P_T(\lambda,t)$ is the measured optical power in the irradiated fiber and $P_T{}^0(\lambda)$ is the optical power of the reference fiber.

3. Environments for use of optical fiber sensing in radiation dosimetry

The possible applications of optical fibers and the optical fiber sensors in radiation monitoring and dosimetry refer to:

1. measurement of the absorbed dose in radiotherapy (Andersen et al., 2002; Jang et al., 2009; Justus et al., 2006) and brachytherapy (Suchowerska et al., 2007);
2. spatial dose distribution in the case of linear electron and proton accelerators for medical treatment (Bartesaghi et al., 2007; Jang et al., 2010a; Lee et al., 2007a);
3. evaluation of beam losses (dose rate, total dose, location) in particle accelerators (Henschel et al., 2004; Intermite et al., 2009; Wulf & Körfer, 2009), beam profiling (Wulf & Körfer, 2009), and the operating conditions of an electron storage ring (Bahrdt et al., 2009; Rüdiger et al., 2008);
4. synchrotron radiation beam profile diagnostics (Byrd et al., 2007 ; Chen et al., 1996);
5. neutron or mixed gamma-ray neutron dosimetry (Bartesaghi et al., 2007a; Jang et al., 2010b);
6. the investigation of isotopic composition of cosmic rays (Connell et al., 1990);
7. radiation dosimetry in computed tomography (Jones & Hintenlang, 2008; Moloney, 2008);
8. distributed radiation dosimetry for beta & gamma rays, and neutrons (Naka et al., 2001);
9. beam profile in the case of free electron lasers (Goettmann et al., 2007) or proton beams (Benoit et al., 2007);
10. remote monitoring of ground water or soil for radioactive contamination (Jones et al., 1993);
11. radiation protection and monitoring of nuclear installations (Magne et al., 2008);
12. monitoring of radioactive waste (Nishiura & Izumi, 2001);
13. reconstruction of the charge particle tracks (Adinolfi et al., 1991; Angelini et al., 1989; Atkinson et al., 1988; Mommaert, 1992; Nakajima et al., 2009 ; Yukihara et al., 2006);
14. the use as transfer detectors for dosimetric calibrations (Tremblay et al., 2010);
15. space dosimetry (Yukihara et al., 2006);
16. tritium detection (Jang et al., 2010c).

In addition, optical fiber-based dosimeters can find in the near future their way in more common environments. One of the main application areas of gamma radiation is in sterilisation, in particular, the sterilisation of medical products. The ability of radiation to kill pathogenic micro-organisms is the basis on which the sterilisation of medical products depends. It is used in a wide variety of products such as hypodermic needles, surgical sutures, blood handling equipment, implant substances and tissues, surgical gloves and utensils, catheters, dental supplies, etc. It is still unknown how exactly the radiation kills micro-organisms, however it is thought to be associated with the damage caused by the radiation to the deoxyribonucleic acid (DNA) of the micro-organism (McLaughlin et al., 1989). The radiation sensitivity of micro-organisms depends on the amount of DNA in the nucleus, but it also depends on a number of other factors, such as the environment they are in. Micro-organisms irradiated in an aerobic environment are more sensitive than those in an anaerobic environment. Also, those in water are more sensitive than those in the dry state. The exact dose of gamma radiation used in the sterilisation of medical products varies for different countries but is usually between 25 kGy and 35 kGy (McLaughlin et al., 1989).

Gamma radiation can be used for a number of different applications within the food industry. Food can be treated to prevent sprouting in onions, garlic and potatoes, to extend

the shelf-life of mushrooms, cherries and strawberries, to eradicate insects in grain and fruit, to kill pathogenic microorganisms in fish and meat, to pasteurize dried herbs and spices, and to delay ripening of fruit and vegetables. Radiation can also be used to prevent the spoilage process, which commonly leads to the rotting of food and wastage. This is due to radiation slowing down the physiological, chemical and biochemical changes occurring in the food and killing micro-organisms and insects. Although radiation does not prevent the drying out of fresh food, its application allows the food to be treated in a sealed package, which prevents both the desiccation process and the microbial re-contamination. Food irradiation treatment depends on the ability of radiation to kill cells and alter the enzyme activities of the food. The killing action of radiation, which inhibits cell division, is used to prevent sprouting, reduce the number of viable micro-organisms on the food, prevent the hatching of insect eggs and larvae, and kill or sterilize the insects in the food. A radiation treatment of between 1 kGy to 7 kGy, depending on the product, can significantly reduce the number of viable pathogenic micro-organisms, e.g. *Salmonella*, *Escherichia coli* and *Lysteria*, which can contaminate food causing serious food poisoning (McLaughlin et al., 1989, O'Keeffe & Lewis, 2009).

A number of other applications for radiation are also being investigated, such as in the treatment of sludge, to reduce the amount of bacteria and infectious micro-organisms, before it may be used as a fertiliser. It is also used in the preservation of ancient objects having historic or artistic value by killing the micro-organisms that can destroy the organic material that the objects are made of or have components of (McLaughlin et al., 1989).

4. Experimental set-up and irradiation conditions

Based on the previous considerations, the best assessment of the color centers' dynamics (the equilibrium between color center generation and the recovery process through photobleaching or heating), for different irradiation conditions (dose-rate, temperature, type of radiation) can be achieved during on-line investigations, by optical absorption measurements. Within such an experimental frame, a broadband spectral analysis of the optical transmission characteristics of the optical fiber is recommended in order to catch the complexity of the phenomena involved. In order to achieve this goal we used a set-up composed of combinations of the equipments listed below:

1. broadband light sources, Analytical Instrument Systems DT 1000 CE stabilized deuterium-tungsten lamp for the UV-visible range or a StellarNet SL1 Tungsten Halogen lamp for spectral measurements in the visible-IR domain;
2. a scientific-grade QE65000, TEC-cooled optical fiber spectrometer from Ocean Optics (1024 x 58 pixels; spectral sensitivity from 200 nm to 1100 nm; 0.065 counts/e- sensitivity; 65% quantum efficiency at 250 nm; 1000:1 S/N ratio; 25000:1 dynamic range/single acquisition; 16 bit resolution; from 8 ms to 15 min. integration time; 3 RMS counts dark noise);
3. a NIR InGaAs TEC-cooled mini spectrometer (1024 pixels; spectral sensitivity from 900 nm to 1700 nm; 4000:1 dynamic range, 12 bit resolution; 4000:1 S/N ration; from 1 ms to 30 s integration time) from StellarNet;

a. NIRX-SR InGaAs, 2 TEC stages, mini spectrometer (1024 pixels, spectral sensitivity from 1600 nm to 2300 nm; 4000:1 dynamic range, 16 bit resolution; from 1 ms to 200 ms integration time) from StellarNet;

b. Avantes optical fiber multiplexers for UV-visible of visible-IR (2 x 8 channels; > 60% optical throughput; > 99% optical repeatability; < 60 ms switching time between adjacent positions).

Several versions of the basic set-up (Sporea & Sporea, 2005) were developed to accommodate various experiments. The overall system is integrated under the National Instruments graphical programming environment and one such experimental implementation is illustrated in Fig. 2 *a*. The experimental instrumentation was used for on-line investigations related to the irradiation effects on silica optical fibers (mostly in the UV range where numerous color centers are developed) and sapphire optical fibers (Sporea & Sporea, 2007; Sporea et al., 2010a; Sporea et al., 2010b). By connecting only one end of the tested optical fiber to different spectrometers, according to the case with or without the use of a multiplexer, the radioluminescent signal was acquired during different types of irradiations. As the temperature plays an important role in recovery of the radiation induced optical absorption some on-line experiments were run by simultaneously irradiating and heating the optical fibers. For gamma-ray irradiation in a cylindrical geometry (the optical fiber, 2 to 5 m long, is coiled and the gamma source is placed in the middle of the circle formed by the fiber) a two sections set-up was used: on the lower level the investigated optical fiber is kept at room temperature, while the optical fiber placed on the higher stage can be electrically heated during the irradiation. A sketch of this mechanical design was presented in Fig. 1 of a previous paper (Sporea et al., 2010a). In that case, the two stages are thermally isolated. For the situation when optical fibers are irradiated by charge particles (electrons or protons) or neutrons, an electrically controlled heater was developed, to rise only locally the temperature of one of the optical fibers, as two short (10 to 15 mm long), similar samples are simultaneously irradiated (Fig. 2 *b*). In this case, each sample is placed into a separate quartz tube, one of these tubes being thermally isolated and coated on the inner side with a heat reflecting layer. In this tube, along with the optical fiber a thermally resistant wire is located parallel to the fiber. By applying a current to this wire the thermally isolated tube is heated. A thermocouple was used to monitor and record in real time the temperature inside the tube. In this way, the optical absorption of both samples is registered in real time, with one of the optical fibers also being subjected to temperature stress.

The set-ups previously detailed were utilized to evaluate the quality of optical fibers suitable for intrinsic or extrinsic radiation monitors (based on optical absorption or radioluminescence) operating at atmospheric pressure. In evaluating materials for alpha particles dosimetry another set-up was designed (Fig. 2 *c*), where the radioluminescence signal is picked-up through a multimode, high UV responsivity optical fiber (Sporea et al., 2010b).

The general conditions for gamma irradiation were described in another paper (Sporea et al., 2010a). In the case of the beta ray irradiation, run at the Linear Accelerator Laboratory of the National Institute for Laser, Plasma and Radiation Physics, the following operating conditions apply: mean electron energy: 6 MeV, the electron beam current: 1 μA, the pulse repetition rate - 100 Hz; the pulse duration - 3,5 μs; the beam diameter - 10 cm; the spot uniformity - +/- 5 %. Proton irradiation was performed at the Tandem irradiation facility of the "Horia Hulubei" National Institute of R&D for Physics and Nuclear Engineering–IFIN-HH, with a beam current of 1 nA, mean dose rate of 200 Gy/s, a total dose of 2.8 MGy, the proton energy of 14 MeV, and the beam diameter of about 3 mm. In some cases, off-line measurements were carried out in order to evaluate the optical absorption recovery either at

room temperature or after heating with a laboratory programmable Memmert oven, controlled over a RS-232 serial interface.

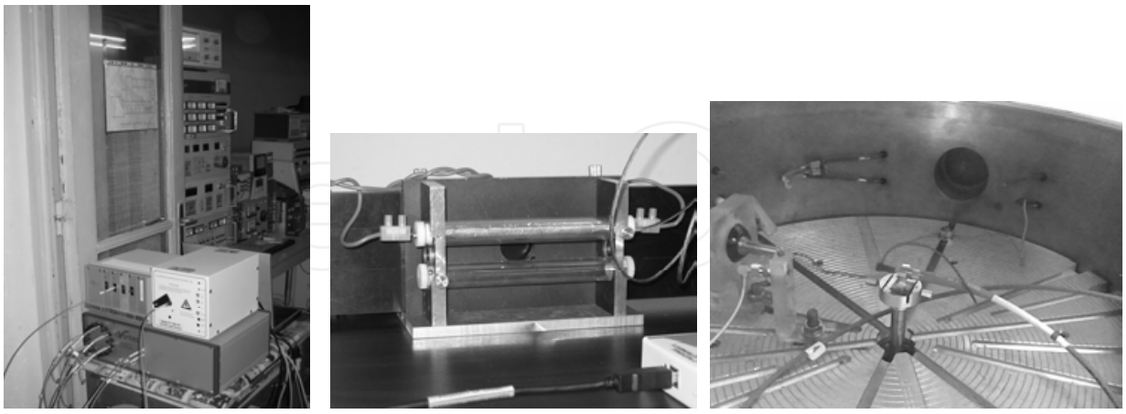

a b c

Fig. 2. Set-ups for the on-line evaluation of irradiation induced optical absorption and radioluminescence: a – the data acquisition and processing system running under LabLIEW graphical programming environment; b – detail of the device used for temperature control of the optical fibers during the irradiation; c – detail of the multimode optical fiber acting as a guiding path of radioluminescence signal generated under alpha particles irradiation (Sporea et al., 2010b).

The two teams jointly investigated, under X-ray irradiation, the characteristics of several extrinsic optical fiber sensors developed at the University of Limerick. Tests in Ireland were done with the ORBITA microfocus X-ray inspection system, while the investigations in Romania were performed with the X-ray micro-tomographic unit developed by Dr. Ion Tiseanu at the National Institute for Laser, Plasma and Radiation Physics. The ORBITA equipment operates within the maximum limits of 0-160 kV, 0- 500 μA. In Romania the sensors were tested with a focused, quasi-monochromatic energy of 17.5 KeV (McCarthy et al., 2011).

5. Optical fiber sensors classification and design

As mentioned in the "Introduction", the use of optical fibers in sensor applications has many advantages over conventional sensors, such as electrochemical and semiconductor sensors. Optical fibers are made of a dielectric material and as such are chemically inert. This makes them very suitable in chemical sensing or in chemically harsh environments. They also provide immunity from electromagnetic interferences and their high electrical isolation makes them suitable for use in lightning protection, high-voltage and medical applications. Optical fibers are also capable of withstanding high temperatures, up to 400 60°C (CeramOptec). These characteristics allow optical fiber sensors to be used in environments not permitted by electrical sensors. Through the use of optical fibers it is possible to have great distances to the measuring point allowing for remote sensing in hostile environments, such as in high-radiation-level areas in the vicinity of a nuclear reactor. The possibility of small, simple interfaces along with lightweight fiber technology results in very appealing sensors. Optical fiber sensors have also been shown to have high sensitivity, large dynamic range along with high resolutions (O'Keeffe, 2008).

The use of plastic optical fibers within the sensor industry is a relatively new technology when compared to glass optical fibers. Plastic optical fibers have been shown to exhibit good transmission in the visible region of the electromagnetic spectrum. Due to the large fiber cross-section of plastic optical fibers, generally a 1 mm core, connecting to the light source and detector is non-problematic. This means that, in contrast to glass optical fibers, no expensive precision components are required for centring the fibers. The large fiber core diameter also means that more light can be transmitted and subsequently incident on the detector, resulting in a higher sensitivity of the sensor. Minor contamination, e.g. dust on the fiber end face, does not result in the complete failure of the sensor system due to its large core diameter. Consequently, fibers can be connected on site in industrial environments with relative ease and without affecting the system. PMMA is also easy to cut, grind and melt and so an uncomplicated process, requiring relatively little time, for processing the end faces is necessary to achieve a clean and smooth surface. Plastic optical fibers are also considered easier to handle when compared to glass optical fibers. Glass fibers tend to break when bent around a small radius, which does not occur with plastic fibers. These fibers are extremely low in cost when compared with glass optical fibers. The properties of PMMA plastic optical fibers result in relatively economical connectors for the system, which further contribute towards a low cost solution (Weinert, 1999).

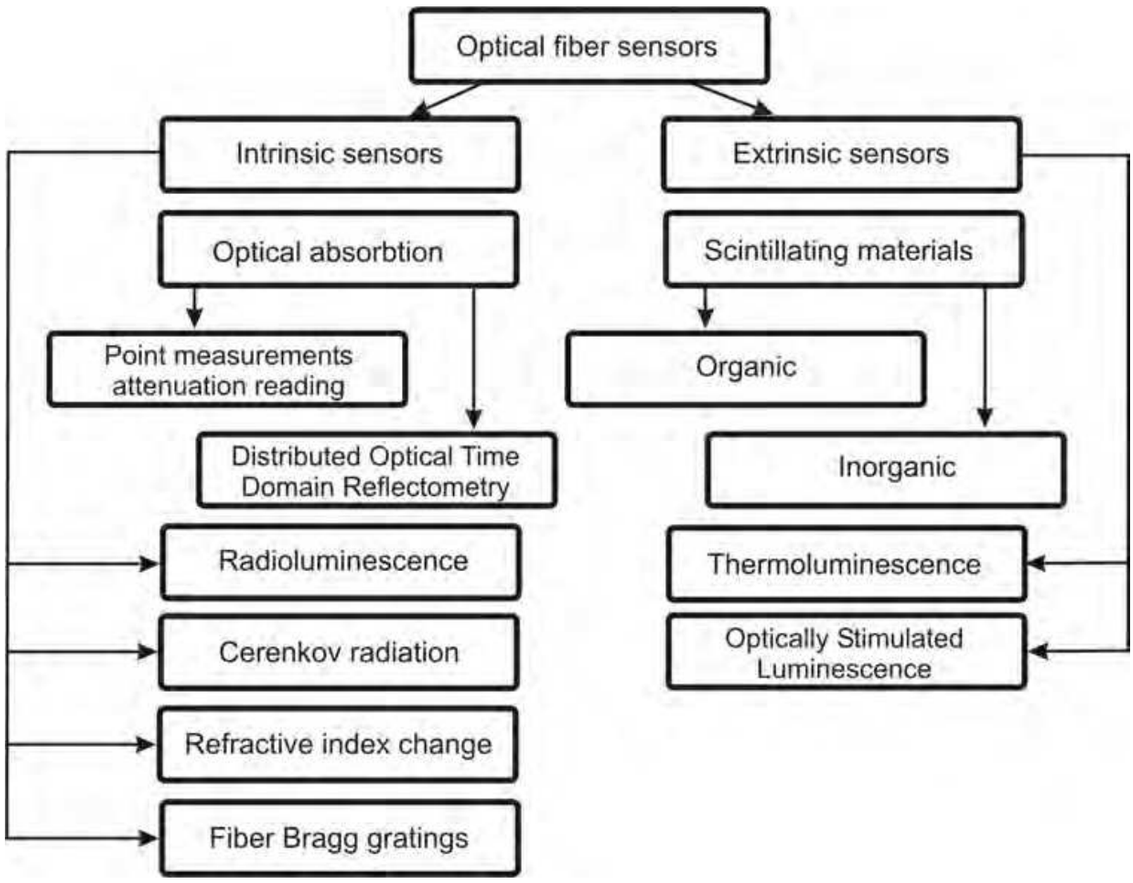

Fig. 3. Classification of the optical fiber sensors for radiation detection according to the operating principle.

Optical fiber sensors can be characterised under two main types: *intrinsic sensors*, where the interaction occurs within the optical fiber itself and *extrinsic sensors*, where the optical fibers are used to guide the light to and from the region where the light interacts with the measurand. Fig. 3 synthesizes the classification of optical fiber-based radiation sensors. Evanescent wave sensors function by causing the light guided in the fiber to couple with the variable to be measured via the evanescent field and have features of both intrinsic and extrinsic devices. It is possible to further classify optical fiber sensors according to the type of modulation to be used (Lopez-Higuera, 1998):

a. Amplitude or intensity sensors detect the amount of light that is a function of the influencing environment. Their ability to use either incoherent or coherent light sources together with simple optical components makes for a low-cost system.
b. Phase or interferometric sensors detect a modulation in phase caused by the measurand. This type of source requires coherent light sources making them a relatively costly system. However, they can provide a very high level of sensitivity.
c. Polarimetric sensors detect a modulation in the polarisation of the light due to the variable to be measured.
d. Spectroscopic sensors detect a modulation in the spectrum of optical radiation due to the influencing variable.

Radiation dosimetry is fundamental to the wide range of radiation processes and as such is the focus of several research endeavours. A number of physical and chemical sensors, which can be subdivided into liquid, solid and gaseous systems, are available to measure ionising radiation and researchers are continually looking for ways to improve the systems, be it increasing the sensitivity, providing real-time measurements or significantly reducing the costs. All these factors are important for providing the optimum radiation dosimeter. In selecting an optical fiber sensor for radiation measurement (dose rate, total dose, point sensor, 1D or 2D sensors) several parameters have to be considered (O'Keeffe et al, 2008):

a. **Mater**ial sensitivity: The ability for radiation to interact with the material is the primary characteristic for any radiation dosimeter. This interaction varies greatly among the different types of radiation dosimeters. The materials utilised in gamma dosimetry must have a high sensitivity to gamma radiation within the dose ranges required for the specific application. Especially for in-vivo medical measurements the sensor has to be sensitive to small dose rate/ total doses, comparable to those involved in radiotherapy.
b. Linearity: The dependency of the sensor out-put signal as function of the input dose/ dose rate. Some applications require a good linearity (no signal saturation) over several decades.
c. The residual signal: It is required that the output signal after its reading (for the case of re-usable sensors such as those based on thermoluminescence or Optically Stimulated Luminescence) to be as small as possible, no cumulative signal from irradiation to irradiation can be accepted or at least this un-read signal has to be reproducible.
d. Post-irradiation fading: The material used as a radiation dosimeter must also show minimum post-irradiation fading. This post-irradiation fading is due to the repair of the physical damage caused to the material during irradiation. Information regarding the irradiation dose is lost if the dosimeter material begins to recover immediately after irradiation.

e. After glow or phosphorescence: in the case of sensors based on radiation induced luminescence a "tail" of the luminescence signal can impinge on the temporal response of the sensor.
f. Time dependence: Many materials also exhibit a time dependence of specific absorbance. This means that it is often required to wait up to 3 h before obtaining an accurate reading. For real time medical applications it is usually important that the dosimeter is fast to measure.
g. Stability and reliability: Stability and reliability of the dosimeter, as with any sensor, are also important. In order to ensure that this can be achieved the dosimeter must be immune to a number of environmental conditions. The effect of humidity and temperature on the dosimeter must be investigated and accounted for. The influence of dose rate on the dosimeter material should also be considered. Immunity to other disturbances, such as those found in electromagnetically harsh environments, is also advantageous for gamma dosimeters as they are often employed in such conditions.
h. Ease of use: For medical applications it is important that the dosimeters are easy to use. For this to be achieved, the system must be easily installed in the area of application without the risk of affecting the measurements. Maintenance should also be minimal. The readout from the dosimeter should be clear and easy to understand. It is also important that the system is low in cost. The availability of clear, easy to implement calibration procedures is an additional advantage.

5.1 Intrinsic optical fiber sensors

Radiation dosimetry based on RIA in gradient index P-doped optical fibers was investigated for ^{60}Co gamma-ray irradiation (dose rates from 0.01 mGy/s to 1.9 Gy/s) and pulsed electrons (total doses of 30 Gy, 100 Gy and 1 kGy). The measurements were carried out at several fixed wavelengths (670 nm, 850 run, 1300 run, and 1550 nm) or spectrally with a spectrum analyser, over the 500 nm to 1700 nm spectral range. In order to be a reliable radiation detector these optical fibers were checked to exhibit high reproducibility, good linearity (over six decades), reduced dose rate dependence (independent over five decades), low fading (a drop of the irradiation induced attenuation of 10 % after two hours and of 14 % after five hours) and small temperature dependence (above 70 ^{0}C the annealing process is significant) and sensitivity to photobleaching (at 10 µW and respectively 10 nW optical power of the laser used to measure the optical absorption no noticeable decrease of the attenuation was observed) (Henschel et al., 1992).
The irradiation induced absorption in doped optical fibers (GeO_2 or P_2O_5, from 12 to 16 mol/%, in the core), under gamma-ray irradiation at low dose rate (1, 0.1 and 0.01 Gy/h, up to a total dose of 1 Gy) was done to evaluate the possible use of such optical fibers as radiation dosimeters. The absorption was monitored during the irradiation (^{60}Co-gamma radiation source of energy 1.25 MeV and Cs-137 radiation source of energy 0.662 MeV) over the wavelength interval 350 nm - 1100 nm (Paul et al., 2009).
As compared to the published data, our investigations focused mostly on the estimation of irradiation effects on special optical fibers, by checking their response in the UV-visible spectral range. We worked with optical fibers such as: solarization resistant; UV-enhanced response; H_2-loaded; or operating in the deep-UV, having a core diameter from 200 µm to 1 mm. We evaluated, using the set-up described under headline 4, optical fibers with different jacket materials: Tefzel, Polyimide or Al (Sporea et al., 2010b). Tests were run under gamma or beta rays, and neutron irradiations. Fig. 4 illustrates some of our results recorded over the

UV-visible spectral range (from 200 nm to 950 nm) for optical fibers irradiated at room temperature.

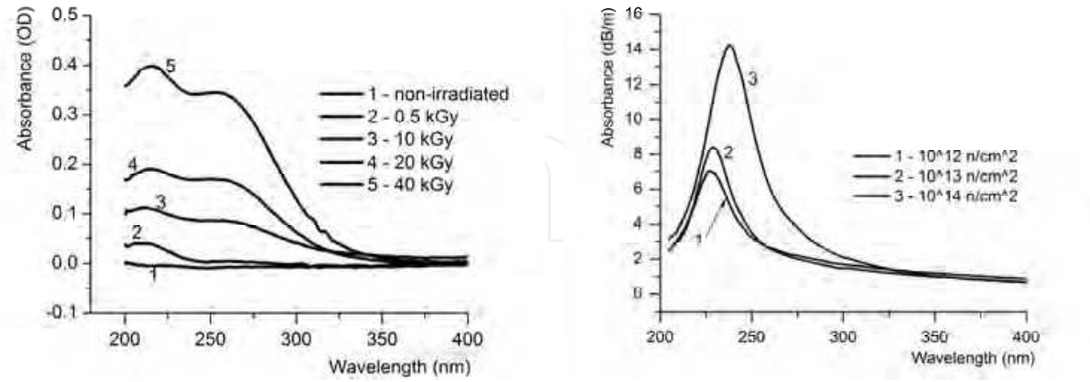

a b

Fig. 4. The changes of the UV optical absorption for: a - 600 µm core diameter, 12 cm long, UV-enhanced, Polyimide jacket optical fiber, irradiated by beta radiation; b - 400 µm core diameter, 10 cm long, solarization resistant, Tefzel jacket optical fiber, subjected to neutron irradiation at three values of the neutron fluences (Sporea et al., 2010b).

The annealing can play an important role in the recovering process of the radiation induced optical absorption. For this reason we run some on-line experiments to evaluate the impact of the ambient temperature during the irradiation process (Fig. 5). The graphs indicate the modifications of the optical attenuation during on-line measurements for a gamma-ray irradiation (dose rate of 36 Gy/min) 400 µm core diameter, UV-enhanced response, H_2-loaded, solarization resistant optical fiber. The difference in the peak maxima results from the coupling losses along the connecting fibers. The change of the optical attenuation is higher for the sample subjected to heating (240 ^{0}C) during the irradiation. Such behaviour can help to select appropriate optical fibers and irradiation conditions in relation to radiation monitoring.

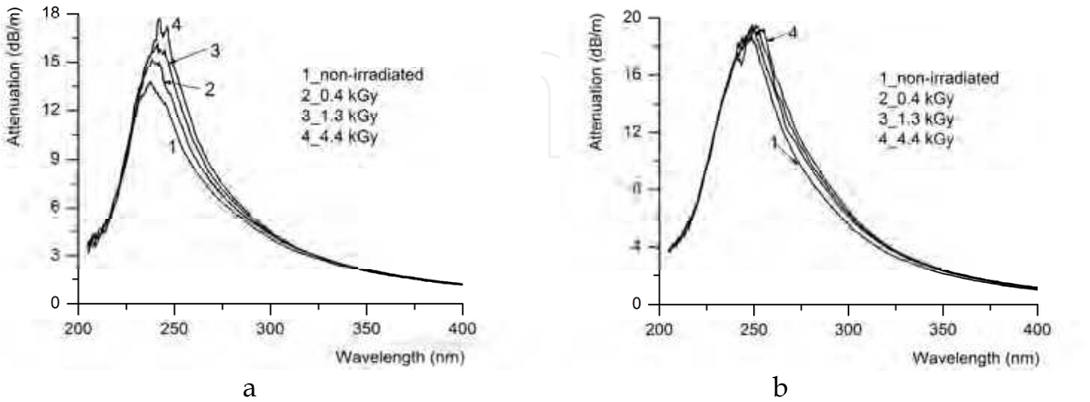

a b

Fig. 5. The influence on the irradiation induced absorption for a 12 cm long, solarization resistant optical fiber: a – heating to 240 ^{0}C is applied to the optical fiber during the irradiation; b – the irradiation is performed at room temperature (Sporea et al., 2010b).

Experimental results (Fig. 4) as well as the corresponding decomposition of the spectral characteristics into Gaussian components (Sporea et al., 2010a) indicate the development of various color centers as the optical fiber is irradiated. In order to estimate the possibility to use UV optical fibers in radiation dosimetry, we measured the change of the optical absorption at two specific wavelengths (Fig. 6 and 7), for different optical fibers, at room temperature, under gamma and beta rays irradiation (Sporea et al., 2010b).
Two wavelengths were monitored in order to optimize the optical fiber as it concerns the radiation sensitivity and linearity of its response with the total dose. The two samples in Fig. 6 *a* exhibit a very good linearity with the total dose if the color center developed at λ = 240 nm is considered. A higher sensitivity can be achieved (in the detriment of the dynamic range) with the same optical fibers, if the measurements are done for λ = 215 nm. The second set of optical fibers (Fig. 6 *b*), being designed for UV applications, are by far less sensitive to gamma irradiation, but they have also a good linear response with the total dose. The results in Fig. 6 indicate a good dynamic range for the investigated optical fibers. Some of the optical fibers tested under gamma-rays were also evaluated under electron irradiation. They showed to have low radiation sensitivity, and a poorer linearity under beta radiation (Fig. 7). The reading at λ = 280 nm for the deep-UV optical fiber designed for laser beam delivery remains almost unchanged with the total dose. The color center produced at λ = 215 nm for the same fiber shows a higher sensitivity and an acceptable linearity up to 40 kGy.

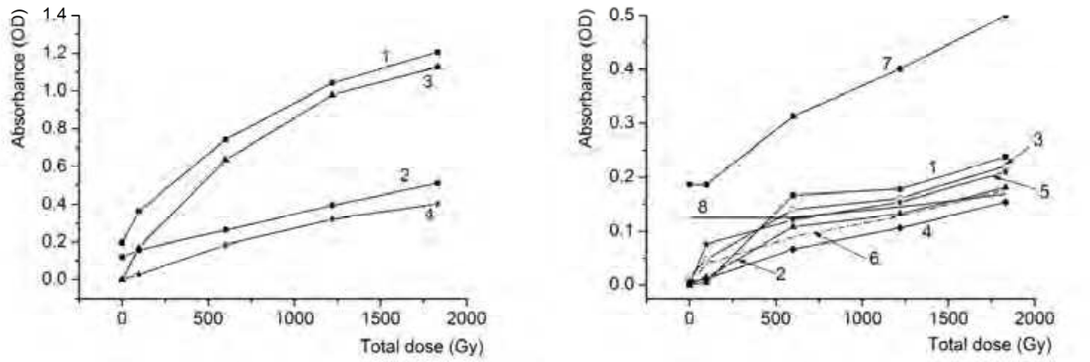

Fig. 6. The optical absorbance as function of the total dose, gamma-ray irradiation (700 Gy/h) for: a – 1 mm core diameter, multimode silica optical fiber, at λ = 215 nm (1) and λ = 240 nm (2); 400 μm core diameter, solarization resistant, Tefzel jacket optical fiber, at λ = 215 nm (3) and λ = 240 nm (4); b – 600 μm core diameter, UV-enhanced, Polyimide jacket optical fiber, at λ = 215 nm (1) and λ = 240 nm (2); 600 μm core diameter, H_2-loaded, Polyimide jacket optical fiber, λ = 215 nm (3) and λ = 240 nm (4); 600 μm core diameter, deep UV-enhanced, Polyimide jacket optical fiber, at λ = 215 nm (5) and λ = 240 nm (6); 400 μm core diameter, deep UV improved for laser delivery optical fiber, at λ = 215 nm (7) and λ = 240 nm (8) (Sporea et al., 2010b).

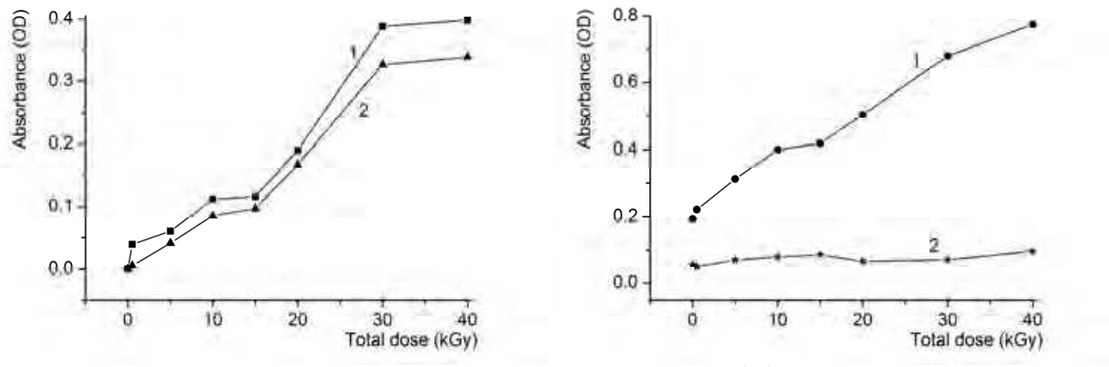

Fig. 7. The optical absorbance as function of the total dose for beta-ray irradiation (6.1 kGy/min) for: a - 600 μm core diameter, deep UV-enhanced, Polyimide jacket optical fiber, at λ = 215 nm (1) and λ = 280 nm (2); b - 400 μm core diameter, deep UV improved for laser delivery optical fiber, at λ = 215 nm (1) and λ = 280 nm (2) (Sporea et al., 2010b).

The RIA induced by X-ray irradiation in multimode P-doped optical fibers (7 wt.% phosphorus concentration in the optical fiber core) was investigated as preliminary studies on the use of such optical fibers to evaluate the total dose (Girard et al., 2011). Measurements were carried out for a total dose up to 3 kGy, at different temperatures (5 ^{0}C; 15 ^{0}C; 25 ^{0}C, 35 ^{0}C and 50 ^{0}C), for dose rates of 1 Gy/s; 10 Gy/s and 50 Gy/ s. The optical absorption was monitored over the 350 nm – 900 nm spectral range. No bleaching of the irradiated optical fibers was noticed and the temperature change under the investigation limits plays a minor role. The highest sensitivity for the irradiation induced absorption was observed in the UV part of the spectrum.

The Irish team explored the possible use of change in the optical absorption in POF under irradiation. Fig. 8 shows the transmission spectrum before the fiber was irradiated and after it was irradiated to 3 kGy of gamma radiation. It is immediately clear that, after exposure to gamma radiation, the transmission is attenuated over the entire visible spectrum. The amount of attenuation depends on the wavelength, with lower wavelengths having a significantly higher attenuation than higher wavelengths (O'Keeffe et al., 2007; O'Keeffe & Lewis, 2009; O'Keeffe et al., 2009a).

The possible use of POFs as radiation monitors is exemplified in reference to Fig. 9, when the peak wavelengths were selected for further analysis. It can be seen that as the wavelengths increase, the rate at which the intensity decreases is reduced. 525 nm shows a rapid decrease in intensity and becomes fully attenuated rapidly. In contrast to this, at 650 nm the intensity, while already low to begin with due to the intrinsically high attenuation in PMMA in this region, decreases at a much slower rate and does not become completely attenuated over the course of the experiment.

The sensitivity of the PMMA fiber to ionizing radiation is directly related to the wavelength and thus by selecting the correct wavelength the fiber can be used to monitor over a wide dose range, selecting 525 nm for low doses with high sensitivity and selecting 650 nm for high doses with lower sensitivity.

Radiation-induced attenuation (RIA) calculations, based on equation 8, were performed on the individual wavelengths to determine the exact sensitivity of the fiber to gamma

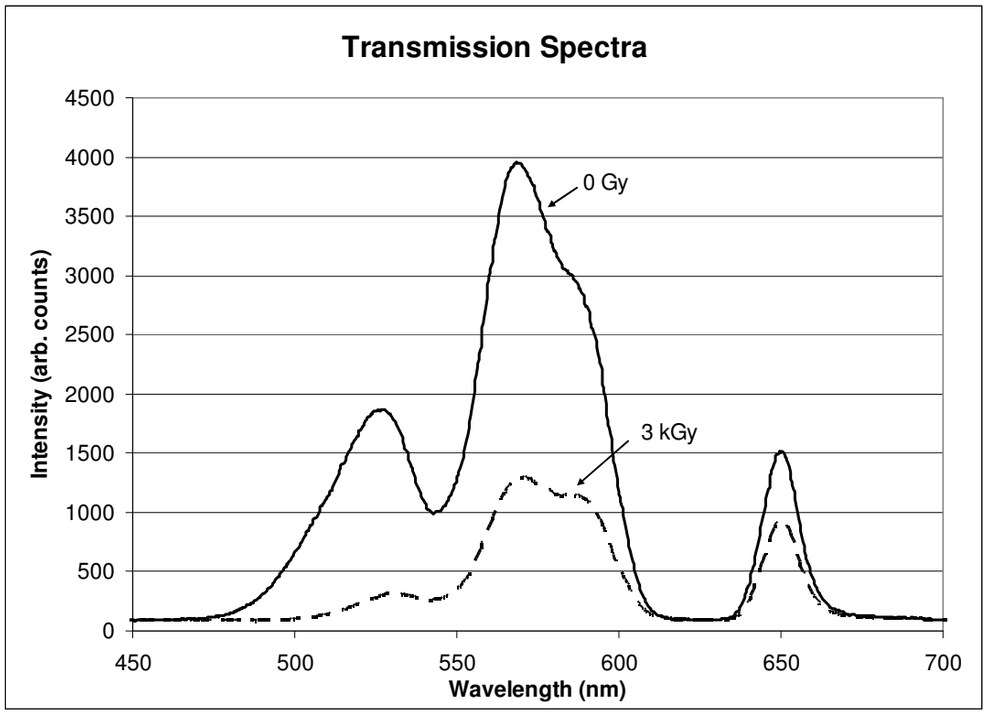

Fig. 8. The transmission of a POF spectra before irradiation and after 3 kGy (O'Keeffe et al, 2009a).

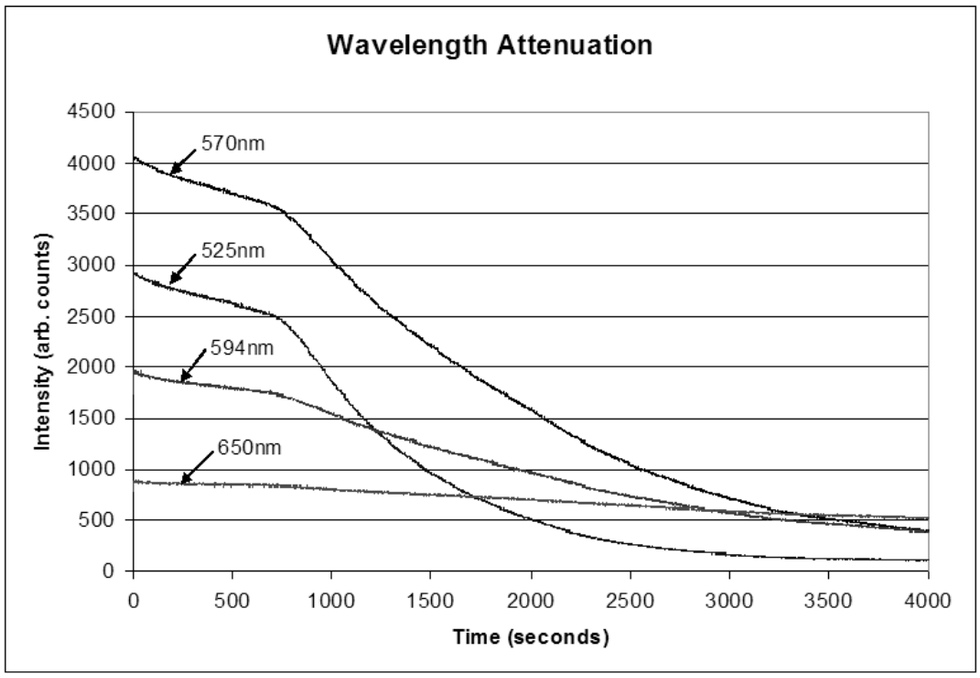

Fig. 9. Intensity of the peak wavelengths over time, as POFs are exposed to gamma radiation (O'Keeffe et al, 2009a).

radiation and the results are presented in Fig. 10 *a*. The wavelength dependence on the RIA sensitivity is evident as the rate of attenuation decreases for increasing wavelength. All the wavelengths exhibit identical characteristics in the RIA with increasing dose. Initially, up to 1 kGy, the RIA increases slowly, followed by significantly higher rate of increase. After this the fiber reaches saturation, whereby the intensity has become completely at that wavelength. The saturation can be seen in Fig. 10 *b*, and indicates the dose range over which the individual wavelengths can monitor. As the wavelength increases the upper-detection limit for that individual wavelength also increases, 4 kGy at 525 nm and 45 kGy at 650 nm (O'Keeffe et al., 2007; O'Keeffe & Lewis, 2009; O'Keeffe et al., 2009a).

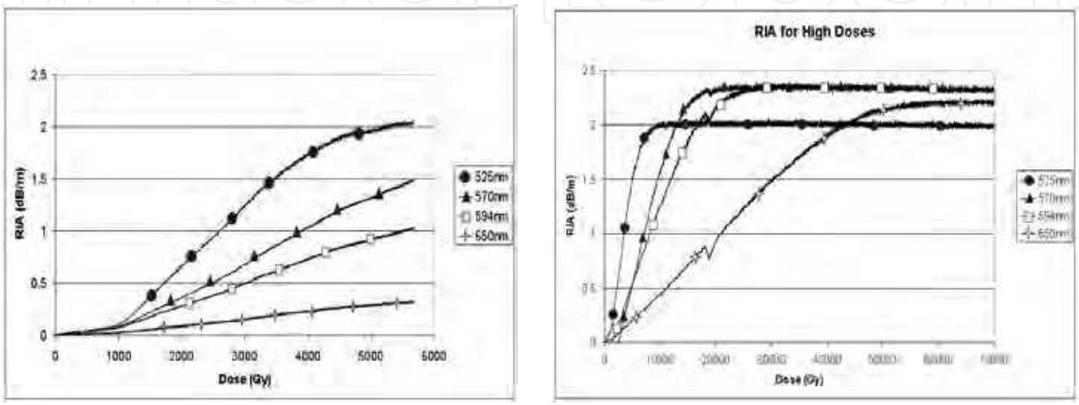

a b

Fig. 10. Radiation-induced attenuation for gamma irradiation; a – total dose up to 5.7 kGy; b – total dose up to 70 kGy (O'Keeffe et al, 2009).

Fig. 11 shows the radiation-induced attenuation at lower radiation doses up to 50 Gy for the two lower peak wavelengths, 525 nm and 570 nm. The determination of lower detection limit of the fiber was limited by the experimental set-up and the high dose rate of the gamma source used, however it can be seen that there is a distinct and immediate increase in the radiation-induced attenuation at these wavelengths. An averaging filter is applied to the data and indicates that beyond 30 Gy there is a steady, quantifiable increase in the radiation-induced attenuation (O'Keeffe et al., 2007; O'Keeffe & Lewis, 2009; O'Keeffe et al., 2009a).

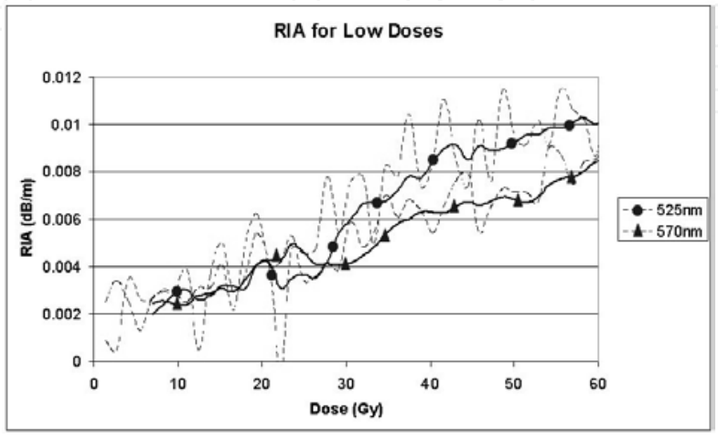

Fig. 11. RIA for low doses of gamma radiation (O'Keeffe et al, 2009a).

Table 1 gives a summary of the sensitivity and dose range of the PMMA fiber for individual wavelengths. It shows that the sensitivity decreases with increasing wavelengths, from 0.6 dBm-1/kGy at 525 nm to 0.06 dBm-1/kGy at 650 nm. The dose range is also dependant on the wavelength as those wavelengths with high sensitivity becoming completely attenuated relatively quickly compared with the higher wavelengths.

Wavelength (nm)	Sensitivity (dBm^{-1}/kGy)	Dosimetry range (kGy)
525	0. 6	0.03 - 4
570	0. 3	0.03 - 10
594	0. 2	0.5 - 12
650	0.06	1 - 45

Table 1. Summary of wavelength dependant sensitivity and dose range.

The radiation induced attenuation of PMMA optical fibers exposed to X-ray radiation, using 6 MV photon energy was reported (O'Keeffe et al, 2009b). The transmission spectra were monitored online and were recorded every two seconds for analysis of attenuation changes as the radiation dose was increased. The results of the RIA calculations are shown in Fig. 12 for two peak wavelengths, 565 nm and 594 nm. There is an immediate and distinct increase in the RIA as the PMMA optical fiber is exposed to the X-ray radiation. The initial results indicate a sensitivity of the fibers to radiation of 0.001 dBm-1/Gy.

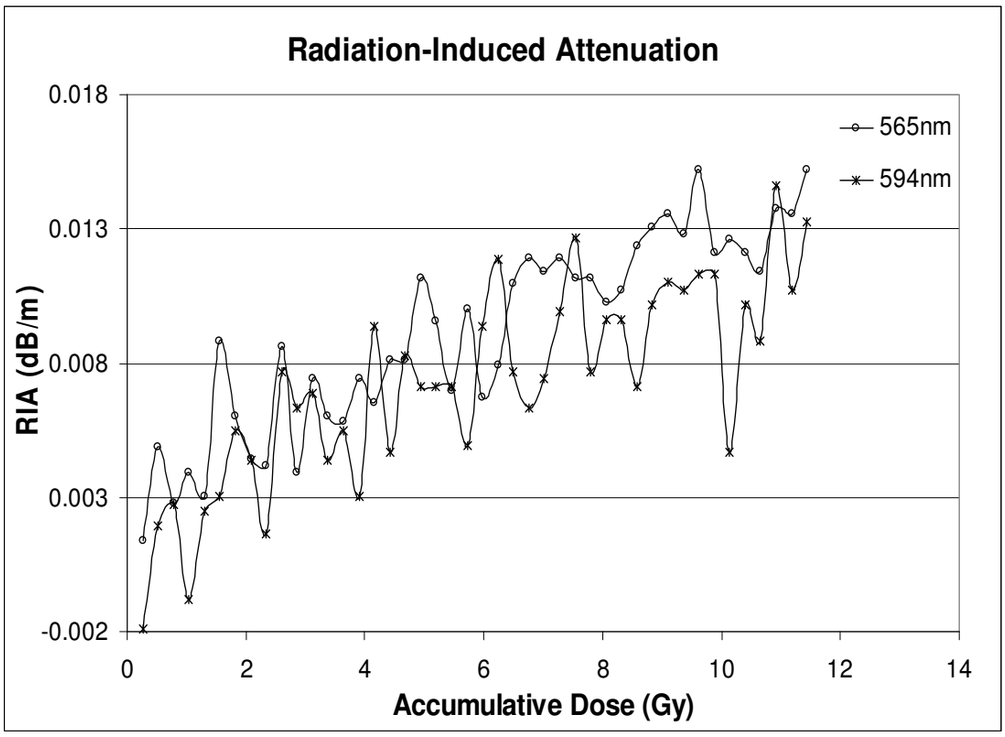

Fig. 12. Radiation Induced Attenuation for two wavelengths, 565nm and 594nm, for POFs under X-ray irradiation (O'Keeffe at al, 2009b).

As the beam losses in particle accelerators have to be checked over long distances a monitoring system, using the principle of Optical Time Domain Reflectrometry (OTDR), was designed for DESY TESLA accelerator (Henschel et al., 2004). The operation of this distributed dosimeter is based on the attenuation induced in optical fibers as they are exposed to radiation associated with machine operation (X-rays, electromagnetic showers). When a short laser pulse is launched into the fiber, some Rayleigh back-scattered optical radiation coming from the fiber sections where color centers are generated by the highly energetic radiation is collected by a detector. From the time of flight and the level of the returned optical radiation pulse a distributed dose mapping can be done, as the pulsed propagation time can be linked to the distance from the laser source of the perturbing non-homogeneities. Within some limits the amount of the detected light can reflect the dose to which the optical fiber segments were exposed. The main limitation of the system is related to the more or less permanent degradation of the optical link transmission during the irradiation. Some solutions to this problem were tested, with not so encouraging results, as for example photobleaching with laser radiation at 830 nm (100 mW CW operation), 670 nm (200 mW/CW), 532 nm (3 W/ CW and 5.5 kW/pulsed).

In the case of P-doped optical fibers, an alternative to extend the operation lifetime of the system can be the thermal annealing (Kuhnhenn et al., 2004). The radiation sensitive optical fiber was subjected to several ^{60}Co irradiation (dose rates between 2.05 to 3.2 Gy/min, total dose of 1000 Gy) - annealing cycles (heating to 400 ^{0}C). A cumulated (after several cycles) residual optical attenuation was observed (about 0.25 dB/m), while the radiation sensitivity of the optical fiber changes very little.

Among the advantages, at least theoretically, of such a system reside in: on-line, distributed dose monitoring; permanent access to difficult to reach locations in complex installations; the possibility to "tune" the sensitivity of the system for specific dose and dose rates, based on the selection of the optical fiber and the interrogation wavelengths used. In order to solve the problem related to the limits imposed by the optical fiber length and the increase in time of the fiber attenuation, an alternative set-up was suggested when the same OTDR units interrogates the optical link from both ends. Even multiple distributed sensors can be operated by the same control instrument (Henschel et al., 2004). Nevertheless, there are some difficulties as it concerns the system performances (the optical fiber radiation sensitivity, the needed information on the exposed optical fiber length, the saturation of the attenuation with total dose). For location where the dose has to be more strictly monitored, a set of local optical fiber dosimeters were designed. In this approach, the attenuation changes with the irradiation dose were evaluated with a LED (λ = 660 nm, for a higher sensitivity) as an interrogation light source, and a set of optical power meters coupled to the LED though connecting optical fibers and segments of radiation sensitive optical fibers, the last ones located in radiation exposed areas.

Apart from standard silica and plastic optical fibers, microstructured optical fibers (MOF) such as photonic crystal fibers (PCF) and random hole optical fiber (RHOF) were tested under irradiation, to assess their radiation hardness or possible use in radiation dosimetry (Wu et al., 2003). In RHOFs the silica core is surrounded by thousands longitudinal channels, having random positions and dimensions. By coating the holes of a RHOF with a phosphorescent material acting as a converter of X-ray or gamma-ray energy to optical radiation, a dose rate monitor can be built, the optical fiber as a whole acting also as a light guide (Alfeeli et al., 2007).

A sensor based on the detection of the Cerenkov radiation produced in a bunch of radiation resistant, high OH-content optical fibers was used to optimize the injection efficiency of the transfer channel between the synchrotron and the storage ring at DELTA. The set-up makes possible a 2D mapping as the time of flight is used to evaluate the location of the Cerenkov radiation produced along the optical fiber, with a longitudinal spatial resolution of 0.2 m corresponding to a delay of about 1 ns between two Cerenkov flashes, while the spatial positioning of the detecting optical fibers assures the localization along the transversal direction (Rüdiger et al., 2008; Wittenburg, 2008). Higher spatial resolution of the Cerenkov radiation-based sensor can be achieved by employing two parallel positioned optical fibers, one used as reference (it is optimized to generate and guide the maximum amount of Cerenkov radiation) and the other one is structured as a sequence of alternating segments of optical fibers similar to the reference fiber and optical fibers having a much higher attenuation. Both optical fibers are coupled to silicon photomultipliers. In this way, if the segments composing the second optical fiber are short enough, by measuring the attenuated signal as compared to the optical signal picked-up by the reference optical fiber, the location of the generated Cerenkov radiation can be identified (Intermite et al., 2009).

A set of four radiation resistant, high-OH content optical fibers, coupled to photomultiplier tubes to detect the Cerenkov radiation, were installed in equidistant radial arrangement along the undulator section of a free electron laser. The position of a wire scanner crossing the electron beam is correlated with the detected Cerenkov radiation, resulting in beam loss, and so, the profile of the beam can be reconstructed by appropriate data processing of the acquired optical signal (Goettmann et al., 2007).

A distributed radiation dosimeter for beta rays, gamma rays and neutrons was designed by using a plastic optical fiber (POF) subjected to irradiation and by detecting the fluorescence and Cerenkov radiation optical signals at both ends of the optical fiber. The time-of-fly technique applied to pulses detected by photomultiplier tubes combined with time-to-amplitude converters and a multichannel analyzer was used to locate the place where the irradiation occurs (Naka et al., 2001). The operating parameters of the equipment (responsivity, resolution) are function of the energy spectrum of the detected radiation, the optical fiber attenuation and degradation, the emission spectrum of the generated optical radiation.

We explored the possible use of sapphire optical fibers in spectroscopic applications in radiation environments and in radiation dosimetry. 25 cm long 425 μm diameter sapphire optical fibers were measured in relation to the radiation induced attenuation (Fig. 13) and radioluminescence, as they were subjected to gamma-ray, proton and neutron irradiation (Sporea & Sporea, 2007). By analyzing the experimental data we noticed the radiation resistance of these optical fibers and the three peaks spectrum of the RL emission under proton irradiation. As the sapphire fibers proved to be immune to radiation (tests were run for gamma-ray up to 530 kGy total dose, for proton up to 2.8 MGy total dose, and for neutron for fluences up to 3.15×10^{13} n/cm^2) we can think to have these optical fibers as real time dose rate monitors, by measuring the RL signal (Fig. 14). Because a small increase of the optical attenuation occurs for λ = 350 nm to 550 nm after irradiation, dosimetric evaluation based on RL can be performed more accurately if the amplitudes of both emission peaks (λ = 440 nm and λ = 690 nm) are considered to correct the green emission measurements. The noisy signal in UV is due to a poor transmission of sapphire under 350 nm. The set-up described in section 4 has the capability to acquire the time dependence of data at selected wavelengths, hence there is the possibility to monitor in real the radioluminescence associated to different centers and to have information on the beam energy.

Another intrinsic type of optical fiber sensor, suggested to be used in particle accelerators for evaluation of very high doses, is based on a Mach-Zehnder interferometer. One of the interferometer arms represents the reference, while the other arm is exposed to irradiation. This second arm is formed by a radiation sensitive optical fiber exhibiting a refractive index change with the radiation dose, and, by combining the coherent radiation traveling along the two arms, a variation of the refractive index produced by the irradiation can be detected (Henschel et al., 2000).

Exploring the radiation induced changes in the refractive index of silica optical fibers a FBG-based dosimeter was suggested, applicable to high radiation doses (10^3 Gy up to 10^5 Gy with an accuracy of at least 10%). Measurements were carried out, at different dose rates, under gamma ray irradiation, assuring a strict control and measurement of the temperature during the irradiation (Krebber et al., 2006). The sensors can be optimized for radiation dosimetry by a careful selection of the optical fiber type and the operating wavelength. It was demonstrated theoretically that FBGs written in photonic crystal fibers (PCF) can achieve a high sensitivity to radiation (at least one order of magnitude) as compared to FBGs produced in bulk material (Florous et al., 2007).

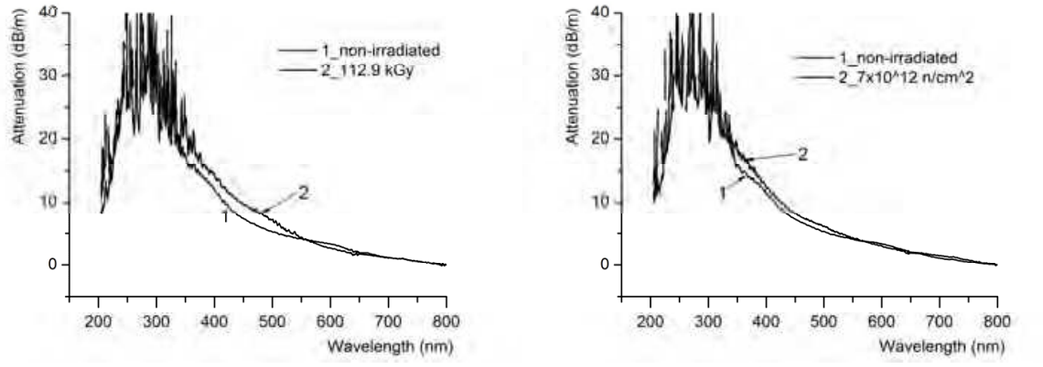

a b

Fig. 13. The changes in the optical attenuation in a 25 cm long, sapphire optical fibers under: a – gamma-ray irradiation; b – neutron irradiation (Sporea & Sporea, 2007).

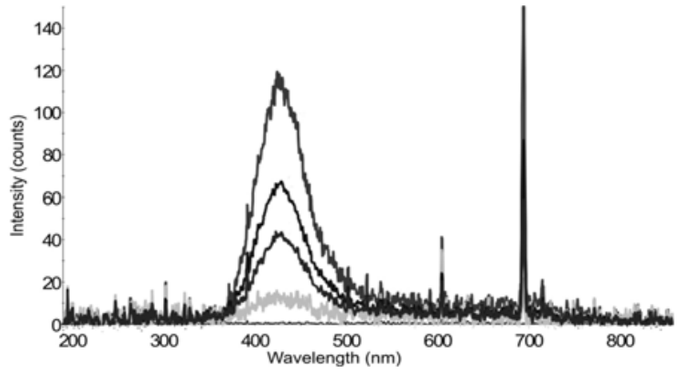

Fig. 14. The radioluminescence emission from a sapphire optical fiber, for proton beam irradiation. The amplitude changes of the RL signal reflects the modifications of the beam current at different irradiation stages (Sporea & Sporea, 2007).

5.2 Extrinsic optical fiber sensors

Point measurements of the absorbed dose in radiotherapy were done by coupling a 10 mm long, 1 mm diameter piece of organic scintillator (Saint Gobain Crystals BCF-20) to a POF acting as light guide for the generated optical radiation. A higher sensitivity of the sensor was obtained by outside coating the scintillating tip by a reflecting TiO_2 layer. The read-out was performed with a photodiode-amplifier system. The device was tested under proton irradiation at a Varian CLINAC 2100C/D accelerator for a 6 MeV energy beam. The amount of the collected optical radiation varied linearly with the dose rate up to 900 cGy/min. The system, acting as a real time instrument, provides within a small volume, high resolution, water equivalent readings, without the need of temperature, humidity or pressure correction (Jang et al., 2009). A similar detecting optical set-up was used to build a 1D array of sensors for high energy proton beam profiling, with scintillating tips spaced 1 cm and respectively 0.5 cm apart, and the light detection with a 10 channel photodiode array (Lee et al., 2007a).

An alternative approach uses a Bicron BC400 scintillating material glued at the end of a PMMA optical fiber and coated with an Al layer, for improved optical radiation collection (Suchowerska et al., 2007). The dimensions of the sensor make possible the limitation of the background optical noise, fluorescence and Cerenkov emission in the optical fiber (less than 0.1 % of the useful signal).

Another optical fiber dosimeter for use in radiotherapy is composed of fused quartz glass doped with Cu^{1+} ions fused to multimode silica optical fiber, which permits the connection to a photomultiplier and a data collection system. Prior to exposure to 6 MV X-rays from a linear accelerator, the radiation detection tip was pre-sensitised under soft X-ray radiation in order to stabilize its responsivity (Justus et al., 2006). To remove the background noise, composed of the native fluorescence in the coupling optical fibers (having a decay time of several ns) and the Cerenkov radiation (emitted in the ps range), and to keep for the dose measurement only the scintillation signal from the Cu^{+}-doped fused quartz optical fiber (lasting several hundreds ms) a gated data acquisition is performed by temporarily selecting the signal to be processed. The measurements carried out indicated the independence of the system response on the dose rate, energy and dose per pulse. Some limits are associated to the long-term stability, degradation under irradiation, directionality of the response (Tanyi et al., 2011).

An array of eight pieces of scintillating optical fibers (BCF-10 type), interlaced with eight pieces of clear optical fibers (BCF-98), both types having a length of 5 mm, and a diameter of 1 mm, was coupled to 16 photomultiplier tubes through a bunch of connecting optical fibers, to form a low resolution, radiation imaging device. The role of the short, clear optical fibers is to collect the perturbing Cerenkov radiation generated into the detecting system during the exposure to charge particle beams. In this way, the Cerenkov "noise" can be subtracted from the signal delivered by the scintillating optical fibers, improving in this way the detecting S/N. The set-up was used to evaluate the depth dose curves in a PMMA (polylmethylmetracrylate) phantom, over a water depth equivalent of 14 cm for proton, and respectively 3 cm for electron irradiation, the spatial resolution being given by the optical fibers spacing of 1 cm (Bartesaghi et al., 2007a). The tissue equivalent response of the detection scheme is given by the polystyrene core of the scintillating optical fibers. A 2D detection scheme based on the same principle was developed (Bartesaghi et al., 2007b). Attempts were made to embed a clear optical fiber into a boron (B_2O_3) doped scintillating tip in order to detect neutrons.

A 1D dosimeter composed of 25 individual sensors, each one fabricated by optically coupling a 4 mm/ 400 μm diameter piece of fused-quartz glass doped with Cu^{1+} ions to a POF, which make possible the transfer of the luminescence signal from the radiation detector tips to a CCD read-out system, was used for mapping the radiation filed in computed tomography - CT (Jones & Hintenlang, 2008).
Another approach to compensate the detected signal collected from the scintillating optical fiber (BCF-60) for the Cerenkov radiation generated in the guiding optical fibers uses a CCD readout scheme in connection to two dichroic beamsplitters. The guiding optical fibers output both the fluorescence signal from the scintillator and the Cerenkov radiation. The scintillating material was selected so that it emits optical radiation in the 500 nm to 600 nm spectral band, while the Cerenkov radiation is predominant in the UV-blue spectral range. One of the beamsplitters reflects towards the CCD array the optical signals with wavelengths lower than 500 nm (mostly the Cerenkov radiation), while the other directs to the detector array the optical radiation between 500 nm and 600 nm. Using a suitable calibration procedure the amount of Cerenkov radiation is subtracted from the two optical signals detected by the CCD and the irradiation dose can then be computed (Frelin & Hintenlang, 2006).
In a recent implementation, the sensing tip consisted of a piece of BGO (Bismuth Germanate – $Bi_4Ge_3O_{12}$) attached to a POF, while the detection was done using a photomultiplier (Seo et al., 2011). The BGO was selected as being a very efficient gamma-ray to light converter.
An alternative design used a polystyrene-based organic scintillator (BCF-60, Saint-Gobain) coupled to a POF in order to separate the Cerenkov signal from the scintillating signal by wavelength discrimination. The optical signal was detected by a CCD camera (Jang et al., 2010a).
An extrinsic, off-line radiation dosimeter for beta radiation based on thermoluminescence in Ge-doped and Al-doped silica optical fibers was suggested (Yaakob et al., 2011). Samples of such optical fibers were exposed to 6, 9, and 12 MeV electron beams, together with classical TLD-100 detectors in order to evaluate the newly proposed detecting materials sensitivity, responsivity, linearity, stability and reproducibility. The optical signal realised upon annealing (done at 400 ^{0}C for 1 h) was read by a Harshaw 4500 TL instrument. Ge-doped optical fibers proved much more sensitive that the Al-doped ones, and exhibit a quite good linearity. The tested optical fibers make repeated usage possible, as no major degradation appeared.
To avoid the optical noise introduced by the Cerenkov radiation in the UV-visible optical spectral range a new type of optical fiber extrinsic dosimeter was proposed. In this approach, a Gd_2O_2S-based scintillator was developed by rare earth ions doping (Pr^{3+}, Yb^{3+} and Nd^{3+}). The scintillating material was optically coupled to a set of optical fibers in order to guide the light to a CCD detector (Takada et al., 1999). In front of the CCD camera the optical signal, guided by the optical fiber bunch, is filtered with an optical high-pass filter. The system has the advantage that the scintillator emits in this case in the IR, hence, the Cerenkov radiation can be cut-down, improving the S/N ratio on the detecting side. To compensate for the radiation induced degradation of the optical fibers transmission the system was complemented with an Optical Time Domain Reflectometer (OTDR). This instrument monitors and localises the increase of the absorption along an optical fiber, of the same type as those used as light guide fibers, which was placed parallel to the connecting optical fibers. In this way, corrections are introduced to compensate for the degradation of the optical links.

Extrinsic optical fiber radiation sensors, proposed in the mid-60s, rely on the Optically Stimulated Luminescence (OSL). The operation of such a detector is based on semiconductor or insulator materials having, in their wide band gap, two additional energy levels. By exposing the material to ionizing radiation, the energy level close to the conduction band is populated, with the number of the trapped electrons being, more or less, proportional to the irradiation dose. At the end of the irradiation process, the material is exposed to an optical radiation at a specific wavelength and the trapped charges are transferred to the second energy level (located also in the band gap, closer to the valence band). By the recombination of these charges, an optical radiation, representing the reading signal of the detector, is emitted (Aznar[a], 2005; Beddar, n.d.; Edmund, 2007). The most common OSL materials used are: MgS:Ce,Sm; SrS:Eu,Sm; NaCl:Cu; KCI:Eu; KBr:In; RbBr:Ti; BbI:In; A-AI2O3; CaS:Ce,Sm; SrS:Ce,Sm (Liu et al., 2008); KBr:Eu (Klein & McKeever, 2008). Such a sensor can exhibit a very low detecting threshold (down to 10 μGy) and a dynamic range over 6 decades (Benoit et al., 2007). Depending on the materials used, the reading optical radiation is in the visible to near-IR spectral range, while the detected optical radiation is mostly in the UV-visible domain. As the two radiations are spectrally separated the same optical fiber can be employed to carry-out both the stimulation signal (from a light source to the ionising radiation detector) and the luminescence one (from the ionising radiation detector towards the optical detector (photomultiplier, CCD, photodiode)), the luminescence material being optically coupled to one end of the signal guiding optical fiber.

An on-line, OSL dosimeter for the evaluation of both dose rate and total dose was developed by optically coupling a solid state dosimeter of carbon doped aluminium oxide (Al2O3:C) to an optical fiber (Andersen et al., 2002). During radiation exposure, some electrons are trapped for a short time in lattice defects of the solid state material, and, as they recombine with holes, a radioluminescence (RL) signal is emitted. In the mean time, additional charges continue to be trapped, as previously described, until an optical radiation stimulus, with an appropriate wavelength laser beam (in this case, λ = 532 nm, 20 mW), realise them and, through recombination with holes, a visible radiation is generated through OSL (Aznar, 2005). Both the excitation light and the detected optical signals (RL & OSL) are guided by the same optical fiber from the laser source and towards the detection/ processing unit. A dichroic beamsplitter is used to couple the stimulation laser radiation to the optical fiber and to separate it from the detected signal, during the detection step. The radioluminescence (RL) signal can be correlated to the irradiation dose rate, while the post-irradiation optically stimulated (OSL) signal can be a measure of the total dose, if appropriate calibrations are performed. That is: the RL signal is increasing with the total dose received, and does not depend on the dose rate, acquired dose history or the radiation quantity. If the measurements are done over well defined time intervals, the change of the RL signal corresponding to each time interval is proportional to the dose rate (Andersen, et al., 2009). The equipment was tested with good results (linearity, sensitivity to Cerenkov radiation, reproducibility, angular dependence) under gamma ray, X rays and electron beam irradiation. For X-ray related applications the best reproducibility values achieved were 1.9 % (RL) and 2.7 % (OSL) at 1 σ, with a good linearity up to 30 mGy air kerma (Aznar et al., 2005).

According to the previously described detecting scheme (RL measurement during the irradiation and OSL data acquisition after the irradiation was stopped), both the dose rate and the total dose can be calculated from the RL signal. Unfortunately, these results are affected by the Cerenkov radiation. A correction can be made as the total dose computed from the RL signal is evaluated against the total dose obtained form the OSL signal, when

no Cerenkov radiation is present. An improvement for this method was proposed when, during the irradiation interval, OSL reading is simultaneously run with the RL signal detection (which in turn is of course accompanied by Cerenkov radiation). In this case, equilibrium has to be established between the filling rate of the trapping levels due to irradiation and their depletion rate produced by optical stimulation. From the acquired data the dose rate and total dose can be derived. The method permits the suppression of the background noise and avoids the saturation of the OSL detector as trapped charges are periodically removed (Gaza et al., 2004). The "dynamic depletion" mechanism was applied also in the case of other OSL materials such as KBr:Eu (Gaza & McKeever, 2006).

The principle of operation discussed above was extended to an array of 15 multiplexed OSL and RL sensors (Magne et al., 2008). In designing such a system several characteristics have to be considered for the validation of the sensor: response linearity, the temperature dependence of the OSL and RL signals, reproducibility of one channel readings and from channel-to-channel, fading (decrease of the read signal occurring between the irradiation and the reading moment).

In designing an OSL sensor aspects related to the dependence of the RL and OSL signals on parameters such as temperature (during the irradiation and optical stimulation) and linear energy transfer – LET (in the case of charge particles: electrons, protons or heavy charged particles – HCP) have to be considered (Edmund, 2007).

A more complex extrinsic radiation dosimeter, capable of evaluating separately gamma-ray and thermal neutrons under a mixed irradiation, was devised (Jang et al., 2010b). It consists of two detectors based on the BCF-20, Saint Gobin scintillating optical fiber coupled through POFs to photomultipliers for the optical radiation detection. In addition, one of the scintillating detectors has a ^{6}Li cap used for the conversion of incoming thermal neutrons energy to alpha particles. The sensor was tested against pure gamma-ray and thermal neutrons irradiation by exposing it, separately, to a ^{60}Co gamma source and ^{252}Cf source of fast neutrons. In the last situation, thermal neutrons were obtained by interposing a 5-cm-thick polyethylene block between the source and the detector. During the gamma irradiation both detectors (with and without the ^{6}Li converter) generated the same amount of optical radiation. In the second experiment, when they were exposed only to a mixed gamma – neutron field, the signal from the detector, which includes also the converting material, provides information on both gamma and neutron irradiation, while the scintillating optical fiber generates optical radiation induced only by the gamma irradiation. By subtracting the second signal from the first one the contribution of thermal neutrons can be deduced. By adding a third, dummy optical fiber, which does not include any scintillating material, the background Cerenkov radiation can be taken into account and the measurement results can be compensated for it (Jang et al., 2011b).

Different types of plastic scintillators are available for gamma, alpha, beta and neutron detection, with some of them having short scintillating constants, or operating under high temperatures (Beddar, Bayramov & Sardarly, 2008).

Detection based on radiation induced luminescence was evaluated for neutron in ZnS-Ag (peak λ = 450 nm), ZnS-Cu (peak λ = 570 nm), $SrAI_20_4$-EuDy (peak λ = 500 nm), and gamma-ray in AI_20_3-Cr, $Eu0_2$, and GdO_2, when such materials were attached at the end of a radiation resistant optical fiber. Such a fiber only has the role in guiding the optical signal to the optical detection part of the sensor (Shikama et al., 2004). Other implementations used LTB:Mn; LTB:Cu and LTB:Cu,Ag,P (Santiago et al., 2009); GaN (Pittet et al., 2009).

Three types of inorganic scintillating material (Gd_2O_2S:Tb, $Y_3Al_5O_{12}$:Ce, and CsI:Tl) fixed with an optical epoxy to the end of a bundle of multimode POFs, used to guide the

scintillating radiation towards a photomultiplier, were tested as a tritium sensors (Jang et al., 2010c). Radioactive tritium emits beta rays, which incident on the scintillating material produce optical radiation in the 455 nm – 550 nm spectral range. As the energy of the beta radiation used is very low, the detecting material thickness was designed to be 0.1 mm.

When using scintillating materials it is of interest to assess the stability and the degradation of their characteristics under irradiation. Tests were carried out on PWO (Lead Tungstate - $PbWO_4$) LSO (Lu_2-SiO_5:Ce), and LYSO ($Lu_{2(1-x)}Y_{2x}SiO_5$:Ce crystals (Mao et al., 2009). Upon irradiation, such scintillating crystals can exhibit an increase of the optical absorption, a decrease of the sensitivity, post irradiation phosphorescence (afterglow), a change of the spatial uniformity of their response to radiation. Similar investigations were done on other inorganic scintillators such as: BGO - $Bi_4Ge_3O_{12}$, GSO - Gd_2SiO_5, CWO - $CdWO_5$ (Seo et al., 2009).

A comparison between an inorganic scintillating material (Al_2O_3:C) and an organic scitillator (BCF-12) reveals their advantages and drawbacks (Beierholm et al., 2009):

a. phosphorescence following the irradiation is present in Al2O3:C;
b. as charge carriers are trapped during the irradiation, Al2O3:C exhibits a memory effect making it suitable for OSL sensors production;
c. Al2O3:C has a higher sensitivity than the organic scintillator, but this parameter changes increases with the total dose;
d. Al2O3:C is sensitive to temperature;
e. the temporal response constitute an advantage for BCF-12 material (3.2 ns luminescence life time) as compared to 35 ms for Al_2O_3:C.

Another design of an extrinsic optical fiber radiation detector is based on a phosphorescent tip fixed at the end of a POF. The fiber is prepared by carefully paring back the outer cable insulation of the PMMA fiber using a special tool, exposing a specific length of the PMMA fiber, as shown in Fig. 15 *a*. The exposed fiber is inserted and secured into a plastic cylinder of known uniform diameter. A plastic sleeve is inserted over the fiber cable to ensure relative centering of the fiber core in the plastic molding housing. Fig. 15 *b* shows the PMMA fiber inserted into the plastic cylinder. Once secured, the next step is to prepare the scintillating phosphor material and epoxy mix. The epoxy is formed by adding a known quantity of hardener to another known quantity of resin. While the epoxy is in a liquidated state, a known amount of scintillating phosphor material is combined with the liquidised epoxy. The next step is to inject the epoxy/scintillating phosphor mix into the sealed cylinder mold and let the mixture harden. After a set period of time, the scintillating coated fiber is removed from its mold. Fig. 15 *c* shows the completed fabrication. The fabrication process is described in more detail elsewhere (McCarthy et al., 2010).

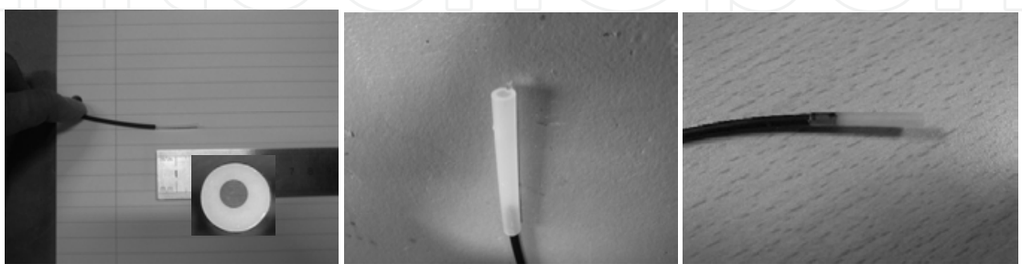

a b c

Fig. 15. The preparation sequences of the phosphorous based extrinsic optical fiber radiation sensor (McCarthy et al., 2010)

The resultant fiber optic sensor described above has been tested and found to respond to excitation from low X-ray energies. The fiber optic sensor connects to a computer controlled fluorescence spectrometer which interprets low levels of light received from the sensor upon excitation from an X-ray source. The fiber optic sensor was exposed to 90 keV X-ray energy and the resultant spectra can be seen below in Fig. 16. The peak wavelength response from the sensor was found to be 544 nm. Sensors using different phosphorus were evaluated under X-ray irradiation in Ireland (broadband X-ray source, energy from 20 keV to 140 keV) and Romania (X-ray quasi-monochromatic 17.5 keV source, I = 800 mA, V = 40 kV), and the emission spectra were recorded with the QE65000 scientific grade spectrometer.

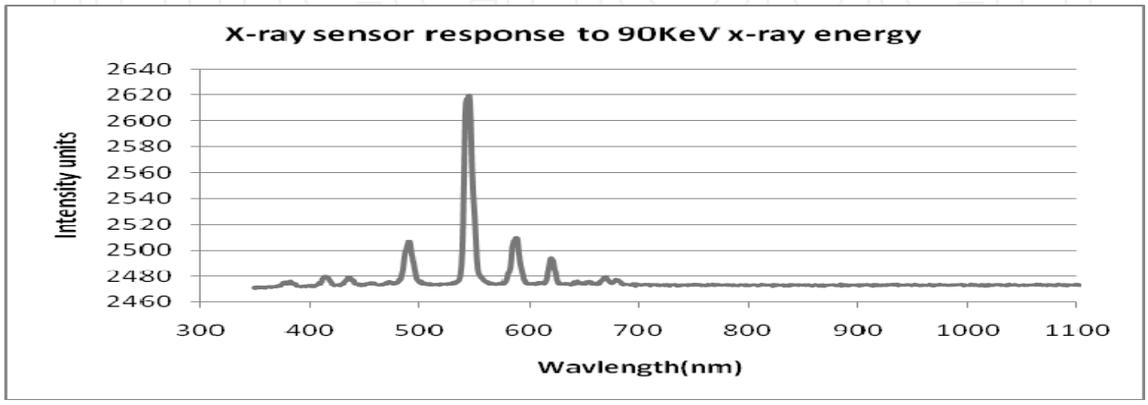

Fig. 16. The spectral response of the X-ray sensor exposed to a 90 keV radiation (McCarthy et al., 2011).

Investigations on the responsivity along the sensor length were carried out by scanning the detector tip along a line parallel to the optical fiber axis (Fig. 17), with a focused (25 μm) X-ray beam (McCarthy et al., 2011).

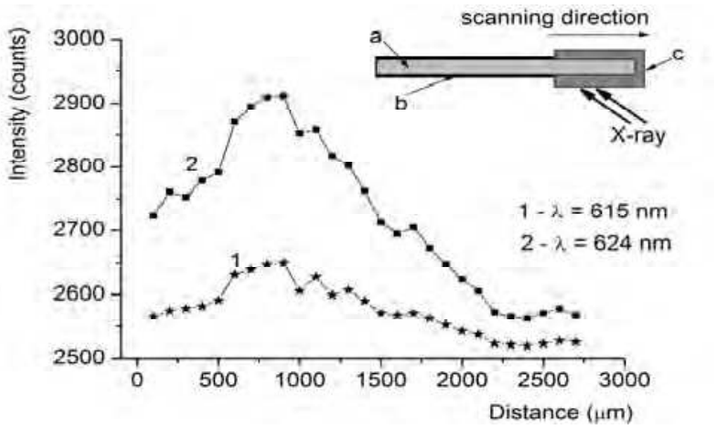

Fig. 17. The spatial responsivity of an extrinsic X-ray sensor for the two peak wavelengths. Insert: a – the POF; b – lightproof jacket; c - phosphorus tip. The focused X-ray beam is scanned along the length of the detecting tip and the profile of the X-ray generated luminescence, as collected by the POSF, is plotted against the distance (McCarthy et al., 2011).

Ge-doped silica optical fibers were investigated as possible thermoluminescence dosimetry (TLD) materials (Hashim et al., 2008). Pieces of 0.8 cm of such optical fibers, carefully measured for their weight (in order to normalize the result to the detector mass) were exposed to X-ray (2 Gy and 10 Gy doses) along with the classical TLD-700 (LiF:Mg,Ti), for comparative evaluation. The signal readout for both materials was done at 300 ^{0}C for 25 s, at a heating cycle rate of 25 ^{0}C/s, with pre-heating at 160 ^{0}C for 10 s. Upon the reading the optical fiber samples were annealed to 400 ^{0}C. The Ge-doped optical fibers have a linear response with the total dose up to 10 Gy. As in the case of other TLD materials, the tested optical fibers exhibit fading (drop of the thermoluminescent signal under lightproof conditions): a decay of 19.7 % after six days storage, as compared to the signal readout after the first 24 h from the irradiation, for the 10 Gy total dose, as compared to the 36.1 % drop for the TLD-700 for the same testing conditions.

Previous studies on commercially available optical fibers (Nokia Cable) used 5 mm long fiber samples irradiated by ^{60}Co gamma radiation at low (from 0.01 Gy to 3 Gy) and high doses (from 4 Gy to 5 kGy). The erase of previously trapped carriers was performed by annealing the samples at temperature from 390 ^{0}C to 490 ^{0}C. The sensor response was compared to a standard TLD-100 dosimeter, as they were subjected to the same irradiation conditions and readings. The peak of the thermoluminescent signal from the optical fiber appeared at about 230 ^{0}C, both for gamma and beta irradiation. Over the entire temperature range, the optical fiber thermally released optical radiation has two peaks, at 400 nm and 575 nm (Espinosa et al., 2006). This investigation did not indicate a significant fading over 15 months of periodic check. The SiO_2 optical fiber presented a higher sensitivity than the TLD-100, by 1.3 times.

In another design, 8 mm long pieces of Ge-doped silica optical fibers were investigated under gamma-ray (^{192}Ir, mean energy 397 keV) and beta (12 MeV energy) irradiation followed by thermoluminescence (TL) reading (Ong et al., 2009). The reported reproducibility is better that 6 %, the sensor having a linear response between 0.2 Gy and 12 Gy for both gamma and beta irradiation. The thermoluminescent signal does not depend on the dose rate and it is angular independent. The fading effect limits the practical use of these optical fibers as thermoluminescent sensors to two weeks.

The same type of optical fibers (Nokia Cable) was evaluated for their possible utilization in OSL dosimetry, as they were exposed to gamma-rays (Espinosa et al., 2011). This optical fiber has a high reproducibility, a low residual signal after several irradiation-reading cycles and, it is estimated from their fading rate, that they can be employed for about six days after the irradiation.

Post irradiation luminescence and the thermoluminescence signals obtained by off-line investigations, from ^{60}Co gamma irradiated COTS optical fibers, are illustrated in Fig. 18 (Sporea et al., 2010b). Depending on the characteristics of the generated optical signal (linearity, reproducibility, sensitivity, etc.) commercially available optical fibers can be incorporated into on-line/off-line radiation detecting schemes, by monitoring the peak value of the emission at specific wavelengths.

Another approach for the design of an extrinsic optical fiber radiation monitor can be developed around Ge-doped silica glass. Figure 19 illustrates the change of the optical absorption and the RL signal as such a glass is irradiated by alpha particles. The optical absorbance measurements were done off-line, while the RL emission was detected on-line using the system described in section 4. In considering the inclusion of such a glass into a real time dose rate meter the same corrections have to be made on the RL signal to

compensate for the decrease of the optical transmission of the glass. Such a detector is a single-use type as far as no recovery of the radiation induced color centers was observed (Sporea et al., 2010b). The optical absorption is linked to the total deposed charge, while the RL signal is a measure of the instant beam current.

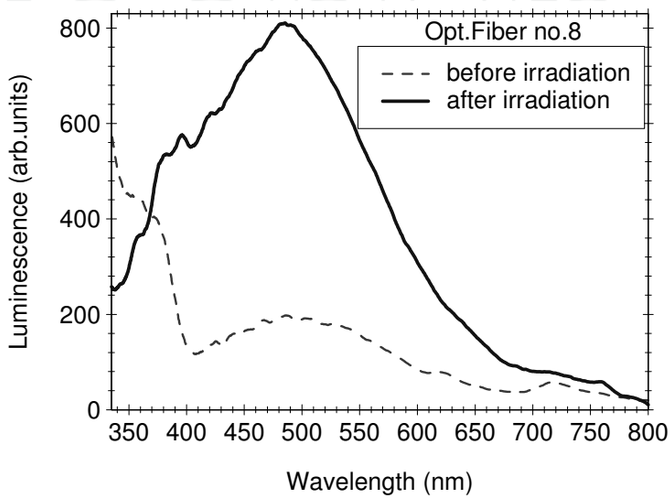

a

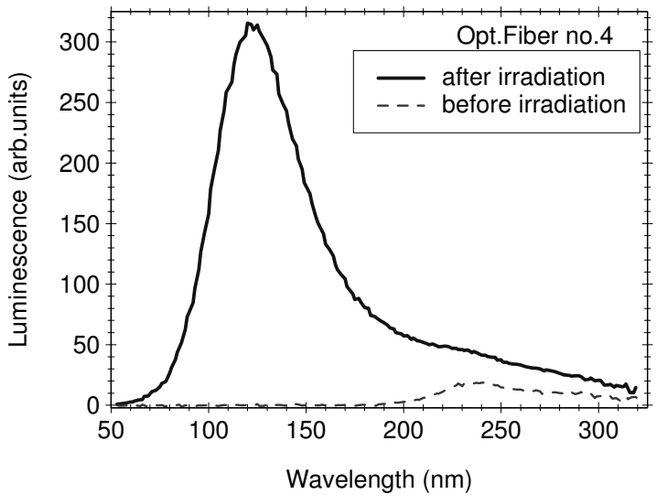

b

Fig. 18. The luminescence (a) and the (b) thermoluminescence signals after ^{60}Co gamma irradiation (total dose 300 Gy, dose rate 158 Gy/h) for: a multimode step-index 400 µm silica core, visible/near-IR optical fiber, with acrylate coating (a); a 600 µm core diameter, deep UV-enhanced, Polyimide jacket optical fiber (b) (Sporea et al., 2010b).

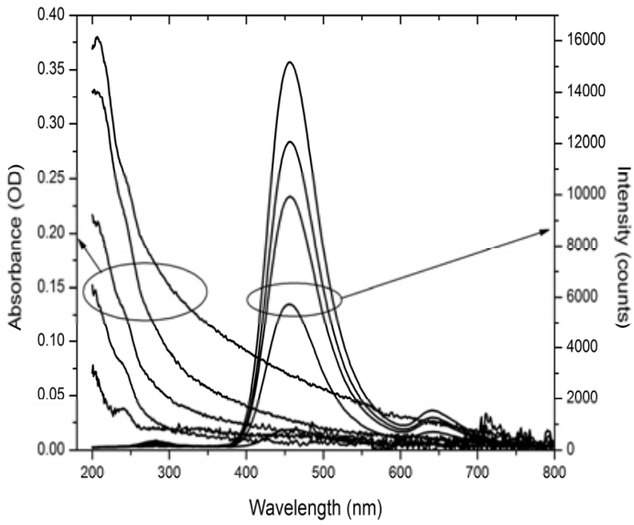

Fig. 19. The changes induced by alpha particle irradiation in a Ge-doped silica glass: a – incease of the optical absorption (left site curves), for various total deposed charge; b – the radioluminescence signal (right site curves), for different instant values of the beam current (Sporea et al., 2010b)

An optical fiber-based system for on-line dosimetry was designed around an optically transparent thermoluminescent glass material containing ZnS nanocrystals and Cu^{11} ions (Huston et al., 1996). In this approach, the thermoluminescent material is optically coupled to a multimode optical fiber. Nd^{3+} ions were additionally included into the ZnS nanocrystals to increase its absorption for the radiation from a semiconductor laser diode emitting 1 W at 807 nm, which is directed through this optical fiber towards the ionizing radiation (the irradiation was done with a ^{60}Co source) detecting material. The laser radiation is used in this case to heat the thermoluminescent material, which generates an optical readout signal. This signal is picked-up by the same optical fiber and is directed towards a photomultiplier by a dichroic beamsplitter combined with some color filters. The luminescence signal has in this application two TL peaks at 160 ^{0}C and 220 ^{0}C. The sensor presents a good linearity with the total dose of doses of medical interest (up to 6 Gy).
Earlier, a multiplexed version was proposed in which the output of a laser diode (λ = 840 nm) coupled to an optical fiber is switched between several "probe" optical fibers. Each such "probe" has fixed at its other end an ionizing radiation detection element. Two such detecting elements were suggested: one formed by a phosphorescent material covered by an absorber and glutted directly to the optical fiber end, or, alternatively, a piece of phosphor, covered by an absorber and mounted to the optical fiber, but isolated with a gap of about 0.1 mm (Jones et al., 1993). As the laser radiation strikes the absorber, its energy is transferred to the phosphor and the thermoluminescent effect appears (at about 400 mW of optical power, reading temperature of 220 ^{0}C – 240 ^{0}C) if the radiation detector was previously irradiated. The generated optical signal is collected by the same system of optical fiber probes and is directed through a wavelength selective beamsplitter towards a photomultiplier. In the first approach, the optical coupling for the thermally generated signal is a better one, but part of

the energy of the laser reading beam is also transferred to the coupling optical fiber. A better sensitivity, from the thermoluminescence point of view, is achieved with the second solution, which has the drawback of a poorer optical coupling for the reading signal. The spectrum of the emitted optical radiation, as well as the temperature of the peak emission, depend on the phosphorus used (in the reported case they are: $CaSO_2$:Mn; CaF_2:Tm; CaF_2:Dy; $CaSO_4$:Dy). The system proved a good linearity over the 1 mGy to 100 Gy range, under ^{60}Co irradiation. In this application it is worth underlining the opportunity to operate with one reading laser and one detector a multitude of multiplexed miniature dosimeters.

6. Future work

Considering the intrinsic characteristics of optical fiber systems: capabilities to work under strong electromagnetic fields; possibility to carry multiplexed signals (time, wavelength multiplexing); small size and low mass; ability to handle multi-parameter measurements in distributed configuration; possibility to monitor sites far away from the controller, their availability to be incorporated into the monitored structure, numerous groups around the world investigated in the past 20 years the possibility to include optical fiber-based devices into radiation monitoring systems. Most of the implementations relay on radiation induced effects such as: increase of the optical absorption on the optical fiber, generation of optical radiation during the irradiation conditions or post irradiation. The chapter evaluates the main solutions promoted for radiation detectors using the optical fiber as a detecting medium or as a light guide for optical signal transmission. The results obtained up to now are encouraging, but the investigative efforts have to continue as it concerns some basic parameters of these devices: sensitivity, linearity, immunity to dose rate and temperature, dynamic range, response time, etc. Besides the main types of optical fibers mentioned in this review, additional research has to be carried out on novel species of optical waveguides (i.e. microstructured optical fibers, photonic optical fibers, mid-IR optical fibers, new scintillating optical fibers). Tests were also carried out on some plastic optical fibers to evaluate their use as total dose monitors considering the increase of their optical absorption at specific wavelengths.

Further investigations have to be done to check for the reproducibility and the stability of the irradiation induced effects for the proposed optical fibers, as well as the possibility to develop re-usable sensors. The level of the fading effect in the case of sensing materials interrogated by thermoluminescnece has to be verified.

For the radioluminescence detection with sapphire optical fibers and doped silica glasses we intent to proceed to the evaluation of the linearity of the emitted signal as function of the beam parameters (beam current, focusing system current, etc.).

The proposed extrinsic POF sensor has to be improved as it concerns the uniformity of the luminescence signals along the sensing tip, as well as the optical coupling of the luminescence emission to the guiding optical fiber. Additionally, we intend to check its linearity for X-rays irradiation, at higher energies. An extension of the research done on this sensor will be the assessment of beta-ray induced luminescence, in conjunction with the evaluation of effects produced by those irradiations (X-ray and beta-ray) on the optical transmission of the coupling optical fibers.

7. Conclusions

An extended review of optical fiber radiation sensors was introduced, with these type of sensors finding applications in various fields, from nuclear industry to radiotherapy, from

space science to particle accelerators. Radiation effects in optical fibers (silica glass, plastic and sapphire) were described along with the classification of the detectors based on intrinsic and extrinsic designs. Examples of authors' experimental results were also included in relation to the tests carried out on silica, plastic and sapphire optical fibers. The evaluation of such optical fibers for the development of radiation monitoring sensors was described.
The chapter emphasis the advantages optical fibers can have in radiation dosimetry: real time measurements (under specific design); small size (able to be used as inside the body or implanted sensors); remote investigations (useful for radiation therapy, particle accelerators, nuclear sites); able to be included into multiplexed or distributed sensor arrays (particle beam diagnostics, monitoring of contaminated sites); susceptible for passive (luminescence, Cerenkov radiation detectors) or active (thermoluminescence, Optically Stimulated Luminescence – OSL) sensing, some of them being water equivalent (an advantage for medical applications).

8. Acknowledgements

The work was done in the frame of the bilateral collaboration existing between the National Institute for Laser, Plasma and Radiation Physics in Bucharest, and the University of Limerick, as part of the COST Action TD1001: *Novel and Reliable Optical Fibre Sensor Systems for Future Security and Safety Applications (OFSeSa)*. The Romanian authors acknowledge the financial support of the Romanian Ministry for Education, Research, Sport and Youth in the frame of the research grant 12084/2008. They also want to thank to their colleagues: Dr. S. Agnello, for providing the Ge-doped silica glass sample, Ms. R. Georgescu and Mr. D. Negut for the gamma irradiation, Dr. C. Oproiu for performing the beta-ray irradiation, Dr. M. Secu for running the luminescence and thermoluminescence measurements, Dr. I. Tiseanu for assisting with X-ray irradiation, Dr. I. Vata for help in doing alpha particles and neutron irradiations. The Irish team wishes to acknowledge the support of the European Commission under the 7th Framework Programme through the 'Marie Curie Re-integration' action of the 'Peoples' Programme, (PERG04-2008-239207).

9. References

Adinolfi, M.; Angelini, C.; Antinori, F.; Beusch, W.; Cardini, A.; Crennell, D.J.; De Vincenzi, M.; Da Vi, C.; Di Paolo, M.; Di Vita, G. ; Duane, A.; Fabre, J.-P.; Flaminio, V.; Frenkel, A.; Gys, T.; Harrison, K.; Lamanna, E. ; Lucchesi¸ D.; Martelloti, G.; McEwen, J.G.; Morrison, D.R.O.; Penso, G.; Petrera, S.; Roda, C.M.A.; Sciubba, A.; Villalobos-Baillie, O. & Websdale, D.M. (1991). Application of a scintillating-fibre detector to the study of short-lived particle, *Nucl. Instr. Met. Phys. Res.*, Vol. A310, (1991), (485-489)

Akchurin, N.; Atramentov, O.; Carrell, K.; Gümüş, K.Z.; Hauptman, J.; Kim, H.; Paar, H.P.; Penzo, A. & Wigmansa, R. (2005). Separation ofscintillation and Cherenkov light in an optical calorimeter, *Nucl. Instr. Met. Phys. Res.*, Vol. A550, (2005), (185-200), doi:10.1016/j.nima.2005.03.175

Alasia, D.; Fernandez Fernandez, A.; Abrardi1, L.; Brichard, B. & Thévenaz, L. (2006). The effects of gamma-radiation on the properties of Brillouin scattering in standard Ge-doped optical fibres, *Meas. Sci. Technol.*, Vol. 17, (2006), (1091–1094), doi:10.1088/0957-0233/17/5/S25

Alessi, A.; Agnello, S.; Sporea, D.G.; Oproiu, C.; Brichard, B. & Gelardi, F.M. (2010). Formation of optically active oxygen deficient centers in Ge-doped SiO_2 by γ- and β-ray irradiation, *J. Non-Cryst. Solids*, Vol. 356, (2010), (275–280), doi:10.1016/j.jnoncrysol.2009.11.016

Alfeeli, B.; Pickrell, G.; Garland, M.A. & Wang, A. (2007). Behavior of random hole optical fibers under gamma ray irradiation and its potential use in radiation sensing applications, *Sensors*, Vol. 7, (2007), (676-688)

Andersen, C.E.; Aznar, M.C.; Bøtter-Jensen, L.; Bäck, S.Å.J.; Mattsson, S. & Medin, J. (2002), Development of optical fibre luminescence techniques for real time in vivo dosimetry in radiotherapy, *Proceedings of the the International Symposium "Standards and codes of practice in medical radiation dosimetry"*, Vol. 2, pp. 353-360, Vienna, November 2002

Andersen, C.E.; Nielsen, S.K.; Greilich, S.: Helt-Hansen, J.; Lindegaard, J.C. & Tanderup, K. (2009). Characterization of a fiber-coupled Al_2O_3:C luminescence dosimetry system for online *in vivo* dose verification during ^{192}Ir brachytherapy, *Med. Phys.*, Vol. 36 No. 3, (March 2009), (708-718), DOI: 10.1118/1.3063006

Angelini, C.; Beusch, W.; Bloodworth, I.J.; Carney, J.N.; Crennell, D.J.; De Vincenzi, M.; Duane, A.; Fabre, J.P.; Fisher, C.M.; Flaminio, V.; Frenkel, A.; Harrison, K.; Hughes, P.; Kinson, J.B.; Lamanna, E.; Leutz, H.; Martellotti, G.; McEwen, J.G.; Morrison, D.R.O.; Penso, G.; Petrera, S.; Quercigh, E.; Roda, C.; Sciubba, A.; Villalobos-Baillie, O.; Votruba, M.F. & Websdale, D.M. (1989). High-resolution tracking with scintillating fibers, *Nucl. Instr. Methods Phys. Res.*, Vol. A277, (1989), (132-137)

Archambault, L. (2005). *Elaboration d'un dosimeter à fibres scintillantes*, PhD Thesis, Faculté des études supérieures de l'Université Laval

Arvidsson, B.; Dunn, K.; Issever, C.; Huffman, B.T.; Jones, M.; Kierstead, J.; Kuyt, G.; Liu, T.; Povey, A.; Regnier, E.; Weidberg, A.R.; Xiang A. & Yef, J. (2009). The radiation tolerance of specific optical fibres exposed to 650 kGy(Si) of ionizing radiation, *JINST 4 P07010*, (2009), doi:10.1088/1748-0221/4/07/P07010

Atkinson, M.N. ; Crennell, D.J.; Fisher, C.M. ; Hughes, P.T.; Kirkby, J.; Fent, J.; Freund, P.; Osthoff, A.; & Pretzl, K. (1988). A high resolution scintillating fiber (SCIFI) tracking device with CCD readout, *Nucl. Instr. Met. Phys. Res.*, Vol. A263, (1988), (333-342)

Aznar, M.C. (2005), *Real-time in vivo luminescence dosimetry in radiotherapy and mammography using Al_2O_3:C*, PhD Thesis, University of Copenhagen, 2005

Aznar, M.C.; Hemdal, B.; Medin, J.; Marckmann, C.J.; Andersen, C.E.; Bötter-Jensen, L.; Andersson, I & Mattsson, S. (2005). In vivo absorbed dose measurements in mammography using a new real-time luminescence technique, *Brit. J.Radiol.*, Vol. 78, (2005), (328–334), doi: 10.1259/bjr/22554286

Bahrdt, J.; Feikes, J.; Frentrup, W.; Gaupp, A.; v. Hartrott, M.; Scheer, M. & Wüstefeld, G. (2009). Cherenkov fibers for beam diagnostics at the metrology light source, *Proceedings of the 23rd Particle Accelerator Conference,* paper TU5RFP029, Vancouver, May 2009

Bartesaghi[a], G.; Conti, V.; Prest, M.; Mascagna, V.; Scazzi, S.; Cappelletti, P.; Frigerio, M.; Gelosa, S.; Monti, A.; Ostinelli, A.; Mozzanica, A.; Bevilacqua, R.; Giannini, G.; Totaro, P. & Vallazza E. (2007). A real time scintillating fiber dosimeter for gamma

and neutron monitoring on radiotherapy accelerators, *Nucl. Instr. Methods Phys. Res., A*, Vol. 572, (2007), (228-230), doi:10.1016/j.nima.2006.10.323

Bartesaghi[b], G.; Conti, V.; Bolognini, D.; Grigioni, S.; Mascagna, V.; Prest, M.; Scazzi, S.; Mozzanica, A.; Cappelletti, P.; Frigerio, M.; Gelosa, S.; Monti, A.; Ostinelli, A.; Giannini, G. & Vallazza E. (2007). A scintillating fiber dosimeter for radiotherapy, *Nucl. Instr. Methods Phys. Res.*, Vol. A581, (2007), (80–83), doi:10.1016/j.nima.2007.07.032

Bayramov, A.A. & Sardarly, R.M. (2008). Applications of plastic sensors, *Fizika*, Vol. CILD XIV, No. 3, (2008), (149-153)

Beddar, S. (n.d). Scintillation dosimetry: Review, new innovations and applications, http://www.aapm.org/meetings/09SS/documents/32Beddar-PlasticDosimeters.pdf

Beierholm, A.R.; Andersen, C.E.; Lindvold, L.R.; Kjær-Kristoffersenc, F. & Medinc, J., A comparison of BCF-12 organic scintillators and Al_2O_3:C crystals for real-time medical dosimetry, *Radiat. Meas.*, Vol. 43, (2008), (898–903), doi:10.1016/j.radmeas.2007.12.032

Benoit, D.; Vaillé, J-R.; Ravotti, F.; Garcia, P. & Dusseau, L. (2007). Optically Stimulated Luminescence Dosimetry, *1st Workshop on Instrumentation for Charged Particle Therapy,* London, May 2007

Berghmans, F. (2006). Ionizing radiation effects on optical components, *NATO Advanced Study Institute, Optical Waveguide Sensing & Imaging in Medicine, Environment, Security & Defence*, Gatineau, October 2006

Berghmans, F.; Brichard, B.; Fernandez Fernandez, A.; Gusarov, A.; Van Uffelen. M. & Girard, S. (2008). An Introduction to Radiation Effects on Optical Components and Fiber Optic Sensors, *Optical waveguide sensing and imaging*, Bock, W.J.; Gannot, I. & Tanev, S., pp. 127-166, Springer Series B: Physics and Biophysics, Dordrecht, The Netherland

Bisutti, J.; Girard, S. & Baggio, J. (2007). Radiation effects of 14 MeV neutrons on germanosilicate and phosphorus-doped multimode optical fibers. *J. Non-Cryst. Solids*, Vol. 353, (2007), (461–465), doi:10.1016/j.jnoncrysol.2006.10.013

Brichard, B.; Borgermans, P.; Fernandez Fernandez, A.; Lammens, K. & Decréton, M. (2001). Radiation effect in silica optical fiber exposed to intense mixed neutron–gamma radiation field, *IEEE T. Nucl. Sci.*, Vol. 48, No. 6, (December 2001), (2069-2073)

Brichard, B.; Fernandez Fernandez, A.; Ooms, H.; Berghmans, F.; Decréton, M.; Tomashuk, A.; Klyamkin, S.; Zabezhailov, M.; Nikolin, I.; Bogatyrjov, V.; Hodgson, E.; Kakuta, T.; Shikama, T.; Nishitani, T.; Costley, A. & Vayakis, G. (2004). Radiation-hardening techniques of dedicated optical fibres used in plasma diagnostic systems in ITER, *J. Nucl. Mater.*, Vol. 329–333, (2004), (1456–1460), doi:10.1016/j.jnucmat.2004.04.159

Brichard, B. & Fernandez Fernandez, A. (2005). Radiation effects in silica glass optical fibers, In: *Short Course Notebook, New Challenges for Radiation Tolerance Assessment*, pp. 95-138, Cap d'Agde, September 2005

Byrd, J.M.; De Santis, S. & Yin, Y. (2007). Fiberoptics-based instrumentation for storage ring beam diagnostics, *Proceedings of 8th European Workshop on Beam Diagnostics and Instrumentation for Particle Accelerator,* pp. 325-327, Venice, May 2007

Calderón, A.; Martínez-Rivero, C.; Matorras, F.; Rodrigo, T.; Sobrón, M.; Vila, I.; Virto, A.L.; Alberdi, J.; Arce, P.; Barcala, J.M.; Calvo, E.; Ferrando, A.; Josa, M.I.; Luque, J.M.; Molinero, A.; Navarrete, J.; Oller, J.C.; Valdivieso, P.; Yuste, C.; Fenyvesi, A. & Molnár, J. (2006). Effects of γ and neutron irradiation on the optical absorption of pure silica core single-mode optical fibres from Nufern, *Nucl. Instr. Met. Phys. Res.*, Vol. A 565, (2006), (599–602), doi:10.1016/j.nima.2006.05.228

Cannas, M.; Lavinia, V. & Roberto, B. (2008). Time resolved photoluminescence associated with non-bridging oxygen hole centers in irradiated silica, *Nucl. Instr. Met. Phys. Res.*, Vol. B, No. 266, (2008), (2945–2948), doi:10.1016/j.nimb.2008.03.144

Caponero, M.A.; Baccaro, Stefania; Donisi, D.; Fabbri, F. & Pillon, M. (2007). Characterisation of FBG sensors under ionizing radiation for high energy physics and space physics, In: *Proceedings of the 10th Conference Astroparticles, Particles and Space Physics, Detectors and Medical Physics Applications*, pp. 533-539, Como, October 2007, doi: 10.1142/9789812819093_0092

Cerenkov, P.A., (1958). Radiation of particles moving at a velocity exceeding that of light, and some of the possibilities for their use in experimental physics, *Nobel Lecture,* December, 1958

Chiodini, N.; Vedda, A.; Fasoli, M.; Moretti F.; Lauria, A.; Cantone, M.-C.; Veronese, I.; Tosi, G.; Brambilla, M.; Cannillo, B.; Mones, E.; Brambilla, G. & Petrovich, M. (2009). Ce doped SiO_2 optical fibers for remote radiation sensing and measurement, *Proceeidngs of Fiber Optic Sensors and Applications VI. SPIE Defense and Security*, Udd, E.; Du, H.H. & Wang, A., Vol. 7316, doi.org/10.1117/12.818507

Connell, J.J.; Binns, W.R.; Dowkontt, P.F.; Epstein, J.W.; Israel, M.H.; Klann, J.; Webber, W.R. & Kish, J.C. (1990). The scintillating isotope experiment: BEVALAC calibrations of the test models, *Nucl. Instr. Methods in Phys. Res.*, Vol. 294, (1990), (335-350)

Deparis, O.; Griscom, D.L.; Mégret, P.; Decréton, M. & Blondel, M. (1997). Influence of the cladding thickness on the evolution of the NBOHC band in optical fibers exposed to gamma radiations, *J. Non-Cryst. Solids*, Vol. 216, (1997), (124-128)

Edmund, J.M. (2007). *Effects of temperature and ionization density in medical luminescence dosimetry using Al_2O_3:C*, PhD Thesis, University of Copenhagen, 2007

Espinosa, G.; Golzarri, J.I.; Bogard, J. & García-Macedo, J. (2006). Commercial optical fiber as TLD material, *Radiat. Prot. Dosim.*, Vol. 119, No. 1-4, (2006), (197-200), doi: 10.1093/rpd/nci564

Espinosa, G. (2011). A study and characterization of the optically stimulated luminescence response of commercial SiO2 optical fiber to gamma radiation, *Rev. Mex. Fís.,*Vol. 57, No. 1, (2011), (30–33)

Fernandez Fernandez, A.; Berghman, F.; Brichard, B.; Decréton, M.; Gusarov, A.I.; Deparis, O.; Mégret, P.; Blondel, M. & Delchambre, A. (2001). Multiplexed fiber Bragg grating sensors for in-core thermometry in nuclear reactors, *Fiber Optic Sensor Technology II, Proc. SPIE*, Vol. 4204, pp. 40-49 , March 2001, doi:10.1117/12.417427

Fernandez Fernandez, A.; Brichard, B., Berghmans, F. & Decréton, M. (2002). Dose-rate dependencies in gamma-irradiated fiber Bragg grating filters, *IEEE T. Nucl. Sci.*, Vol. 49, No. 6, (December 2002), (2874-2878), doi: 10.1109/TNS.2002.805985

Fernandez Fernandez, A.; Brichard, A. & Berghmans, F. (2003). In situ measurement of refractive index changes induced by gamma radiation in germanosilicate fibers,

IEEE Photonic Tech. L., Vol. 15, No. 10, (October 2003), (1428-1430), doi: 10.1109/LPT.2003.818247

Florous, N.J.; Saitoh, K.; Murao, T. & Koshiba, M. (2007). Radiation dose enhancement in photonic crystal fiber bragg gratings: towards photo-ionization monitoring of irradiation sources in harsh nuclear power reactors, *Quantum Electronics and Laser Science Conference*, *QELS '07*, Baltimore, 2007, doi: 10.1109/QELS.2007.4431290

Friebele, E.J. (1991). Correlation of single mode fiber fabrication factors and radiation response, *Naval Research Laboratory _NRL_ Final Report No. NRL/MR/6505_92-6939*, November 1991

Frelin, A.-M.; Fontbonne, J.-M.; Ban, G.; Batalla, A.; Colin, J.; Isambert, A.; Labalme, M.; Leroux, T. & Vela, A. (2006). A new scintillating fiber dosimeter using a single optical fiber and a CCD camera, *IEEE T. Nucl. Sci*., Vol. 53, No. 2, (June 2006), (1113-1117), doi:10.1109/TNS.2006.874931

Gaza; R.; McKeever, S.W.S.; Akselrod, M.S.; Akselrod, A.; Underwood, T.; Yoder, C.; Andersen, C.E.; Aznar, M.C.; Marckmann, C.J. & Bötter-Jensen, L. (2004). A fiber-dosimetry method based on OSL from Al_2O_3: C for radiotherapy applications, *Radiat. Meas.*, Vol. 38, (2004), (809–812), doi:10.1016/j.radmeas.2003.12.004

Gaza, R. & McKeever, S.W.S. (2006). A real-time, high-resolution optical fiber dosimeter based on optically stimulated luminescence (OSL) of KBr:Eu, for potential use during the radiotherapy of cancer, *Radiat. Prot. Dosim.* (2006), Vol. 120, No. 1–4, (14–19), doi:10.1093/rpd/nci603

Girard[a], S.; Keurinck, J.; Boukenter, A.; Meunier, J.-P.; Ouerdane, Y.; Azaïs, B.; Charre, P. & Vié, P. (2004). Gamma-rays and pulsed X-ray radiation responses of nitrogen-, germanium-doped and pure silica core optical fibers, *Nucl. Instr. Met. Phys. Res.*, Vol. B215, (2004), (187–195), doi:10.1016/j.nimb.2003.08.028

Girard[b], S.; Keurinck, J.; Ouerdane, Y.; Meunier, J.-P. & Boukenter, A. (2004). γ-rays and pulsed X-ray radiation responses of germanosilicate single-mode optical fibers: influence of cladding codopants, *J. Lightwave Technol.*, Vol. 22, No. 8, (2004), (1915 – 1922), doi: 10.1109/JLT.2004.832435

Girard, S.; Vincent, B.; Ouerdane, Y.; Boukenter, A.; Meunier, J.-P. & Boudrioua, A. (2005). Luminescence spectroscopy of point defects in silica-based optical fibers, J. Non-Cryst. Solids, Vol. 351, (2005), (1830–1834), doi:10.1016/j.jnoncrysol.2005.04.043

Girard, S.; Ouerdane, Y.; Boukenter, A. & Meunier, J.-P. (2006). Transient radiation responses of silica-based optical fibers: influence of modified chemical-vapor deposition process parameters, J. Appl. Phys., Vol. 99, (2006), doi: 10.1063/1.2161826

Girard, S.; Ouerdane, Y.; Origlio, G.; Marcandella, C.; Boukenter, A.; Richard, N.; Baggio, J.; Paillet,P.; Cannas, M.; Bisutti, J.; Meunier,J.-P. & Boscaino, R. (2008). Radiation effects on silica-based preforms and optical fibers—I: experimental study with canonical samples, *IEEE T. Nucl. Sci*., Vol. 55, No. 6, (December 2008), (3473-3482), doi: 10.1109/TNS.2008.2007297

Girard, S.; Marcandella, C.; Origlio, G.; Ouerdane, Y.; Boukenter, A. & Meunier, J.-P. (2009). Radiation-induced defects in fluorine-doped silica-based optical fibers: Influence of a pre-loading with H_2, *J. Non-Cryst. Solids*, Vol. 355, (2009), (1089–1091), doi:10.1016/j.jnoncrysol.2008.11.035

Girard, S. & Marcandella, C. (2010). Transient and Steady State Radiation Responses of Solarization-Resistant Optical Fibers, *IEEE T. Nucl. Sci.,* Vol. 57, No. 4, (2049 – 2055), doi: 10.1109/TNS.2010.2042615

Girard, S.; Ouerdane, Y.; Marcandella, C.; Boukenter, A.; Quenard, S. & Authier, N. (2011). Feasibility of radiation dosimetry with phosphorus-doped optical fibers in the ultraviolet and visible domain, *J. Non-Cryst. Solids*, Vol. 357, (2011), (1871–1874), doi:10.1016/j.jnoncrysol.2010.11.113

Goettmann, W.; Wulf, F.; Körfer, M. & Kuhnhenn, J. (2005). Beam loss position monitor using Cerenkov radiation in optical fibers, *Proceedings of the 7th European Workshop on Beam Diagnostics and Instrumentation for Particle Accelerators*, pp. 301-303, Lyon, June 2005

Goettmann, W.; Körfer, M. & Wulf, F. (2007). Beam profile measurement with optical fiber sensors at FLASH, *Proceedings of 8th European Workshop on Beam Diagnostics and Instrumentation for Particle Accelerator,* pp. 123-125, Venice, May 2007

Griscom, D.L.; Golant, K.M.; Tomashuk, A.L.; Pavlov, D.V. & Tarabrin, Yu.A. (1996). γ-radiation resistance of aluminum-coated all-silica optical fibers fabricated using different types of silica in the core, *Appl. Phys. Lett.*, Vol. 69, (1996), (322-324)

Gusarov[a], A.I.; Starodubov, D.S.; Berghmans, F.; Deparis, O.; Defosse, Y.; Fernandez Fernandez, A.; Decréton, M.; Mégret, P. & Blondel, M. (1999). Comparative study of MGy dose level g-radiation effect on FBGs written in different fibres, presented at *OFS-13*, Kyongju, April 1999

Gusarov[b], A. I.; Berghmans, F.; Deparis, O.; Fernandez Fernandez, A.; Defosse, Y.; Mégret, P.; Décreton, M. & Blondel, M. (1999), High total dose radiation effects on temperature sensing fiber bragg gratings, *IEEE Photon. Tech. L.*, Vol. 11, No. 9, (September 1999), (1159-1161)

Gusarov, A.; Fernandez Fernandez, A.; Vasiliev, S.; Medvedkov, O.; Blondel, M. & Berghmans, F. (2002). Effect of gamma-neutron nuclear reactor radiation on the properties of Bragg gratings written in photosensitive Ge-doped optical fiber, *Nucl. Instr. Met. Phys. Res.*, Vol. B187, (2002), (79-86)

Gusarov[a], A.; Vasiliev, S.; Medvedkov, O.; Mckenzie, I. & Berghmans, F. (2008). Stabilization of fiber Bragg gratings against gamma radiation, *IEEE T. Nucl. Sci.*, Vol. 55, No. 4, (2008), 2205 – 2212, doi: 10.1109/TNS.2008.2001038

Gusarov[b], A.; Chojetzki, C.; Mckenzie, I.; Thienpont, H. & Berghmans, F. (2008). Effect of the fiber coating on the radiation sensitivity of type I FBGs, *IEEE Photon. Tech. L.*, Vol. 20, No. 21, (November, 2008), (1802-1804), doi: 10.1109/LPT.2008.2004699

Gusarov, A.; Brichard, B. & Nikogosyan, D.N. (2010). Gamma-radiation effects on Bragg gratings written by femtosecond UV laser in Ge-doped fibers, *IEEE T. Nucl. Sci.*, Vol. 57, No. 4, (2010), (2024 – 2028), doi: 10.1109/TNS.2009.2039494

Hanafusa, H.; Hibino, Y. & Yamamoto, F. (1986). Drawing condition dependence of radiation-induced loss in optical fibres, *Electron. Lett.*, Vol. 22, No. 2, (1986), (106-108).

Hashim, S.; Ramli, A.T.; Bradley, D.A. & Wagiran,, H. (2008). The thermoluminescence response of Ge-doped optical fibers to X-ray photon irradiation, *J. Fiz. UTM.*, Vol. 3, (2008), (31-37)

Henschel, H.; Köhn, O. & Schmidt, H.U. (1992). Optical fibres as radiation dosimeters, *Nucl. Instr. Met. Phys. Res.*, Vol. B69, (1992), (307-314)

Henschel, H.; Körfer, M.; Wittenburg, K. & Wulf, F. (2000). Fiber optic radiation sensing systems for TESLA, *TESLA Report No. 2000-26*, September 2000

Henschel, H.; Körfer, M.; Kuhnhenn, J.; Weinand, U. & Wulf, F. (2004). Fibre optic radiation sensor systems for particle accelerators, *Nucl. Instr. Met. Phys. Res.*, Vol. A526, (2004), (537–550), doi:10.1016/j.nima.2004.02.030

Huston, A.L.; Justus, B.L. & Johnson, T.L. (1996). Fiber-optic-coupled, laser heated thermoluminescence dosimeter for remote radiation sensing, *Appl. Phys. Lett.*, Vol. 68, No. 24, (June 1996), (3377-3379)

Ichikawa, T., Mechanism of radiation-induced degradation of poly(methyl methacrylate) -- temperature effect, *Nucl. Instr. Met. Phys. Res. Section B: Beam Interactions with Materials and Atoms*, Vol. 105, No. 1-4, (1995), (150-153), doi:10.1016/0168-583X(95)00534-X

Intermite, A.; Putignano, M. & Welsch, C. P. (2009). Feasibility study of an optical fiber sensor for beam loss detection based on a SPAD array, *Proceedings of 9th European Workshop on Beam Diagnostics and Instrumentation for Particle Accelerators*, pp. 228-230, Basel, May 2009

Jang, K.W.; Cho, D.H.; Shin, S.H.; Yoo, W.J.; Seo, J.K.; Lee, B.; Kim, S.; Moon, J.H.; Cho, Y.-H. & Park, B.G. (2009). Characterization of a Scintillating Fiber-optic Dosimeter for Photon Beam Therapy, *Opt. Rev.*, Vol. 16, No. 3, (2009), (383–386)

Jang[a], K.W.; Cho, D.H.; Yoo, W.J.; Seo, J.K.; Heo, J.Y.; Lee, B.; Cho, Y.-H.; Park, B.G.; Moon, J.H. & Kim, S. (2010). Measurement of Cerenkov light in a fiber-optic radiation sensor by using high-energy photon and electron beams, *J. Korean Phys. Soc.*, Vol. 56, No. 3, (March 2010), (765-769), doi: 10.3938/jkps.56.765

Jang[b], K.W.; Yoo, W.J.; Park, J. & Lee, B. (2010). Development of scintillation-fiber sensors for measurements of thermal neutrons in mixed Neutron-gamma fields, *J. Korean Phys. Soc.*, Vol. 56, No. 6, (June 2010), (1777-1780), DOI: 10.3938/jkps.56.1777

Jang[c], K.W.; Cho, D.H.; Yoo, W.J.; Seo, J.K.; Heo, J.Y.; Park, J.-Y. & Lee, B. (2010). Fiber-optic radiation sensor for detection of tritium, *Nucl. Instr. Methods Phys. Res.*, doi:10.1016/j.nima.2010.09.060

Jang[a], K.W.; Yoo, W.J.; Seo, J.K.; Heo, J.Y.; Moon, J.; Park, J.-Y.; Kim, S.; Park, B.G. & Lee, B. (2011). Measurements and Removal of Cerenkov light generated in scintillating fiber-optic sensor induced by high-energy electron beams using a spectrometer, *Opt. Rev.*, Vol. 18, No. 1, (2011), (176–179)

Jang[b], K.W.; Lee, B. & Moon, J.H. (2011). Development and characterization of the integrated fiber-optic radiation sensor for the simultaneous detection of neutrons and gamma rays, *Appl. Radiat. Isotopes*, Vol. 69, (2011) (711–715), doi:10.1016/j.apradiso.2011.01.009

Jones, A.K. & Hintenlang, D. (2008). Potential clinical utility of a fiber optic-coupled dosemeter for dose measurements in diagnostic radiology, *Radiat. Prot. Dosim.*, Vol. 132, No. 1, (2008), (80–87), doi:10.1093/rpd/ncn252

Jones, S.C.; Hegland, J.E.; Hoffman, J.M. & Braunlich, P.F. (1990). A fibre-optic TLD microprobe for remote in-vivo radiotherapy dosimetry, *Radiat. Prot. Dosim.*, Vol. 34, No. 1/4, (1990), (279-282)

Jones, S.C.; Sweet, J.A.; Braunlich, P.; Hoffman, J.M. & Hegland, J.E. (1993). A remote fibre optic laser TLD system, *Radiat. Prot. Dosim.*, Vol. 47, No. 1/4, (1993), (525-528)

Justus, B.L.; Falkenstein, P.; Huston, A.L.; Plazas, M.C.; Ning, H. & Miller, R.W. (2006). Elimination of Cerenkov interference in a fibre-optic-coupled radiation dosimeter, *Radiat. Prot. Dosim.*, Vol. 120, No. 1–4, (2006), (20–23), doi:10.1093/rpd/nci525

Klein, D.M. & McKeever, S.W.S. (2008). Optically stimulated luminescence from KBr:Eu as a near-real-time dosimetry system, *Radiat. Meas.*, Vol. 43, (2008), (883 – 887), doi:10.1016/j.radmeas.2008.01.015

Krebber, K., Henschel, H. & Weinand, U. (2006). Fibre Bragg gratings as high dose radiation sensors?, *Meas. Sci. Technol.*, Vol. 17, (2006), (1095–1102), doi:10.1088/0957-0233/17/5/S26

Kuhnhenn, J.; Henschel, H.; Köhn, O. & Weinand, U. (2004). Thermal annealing of radiation dosimetry fibres, *Proceedings RADECS 2004*, pp. 39-42, Madrid, September 2004

Kuhnhenn, J. (2005). Radiation tolerant fibres for LHC controls and communications, *5th LHC Radiation Workshop*, CERN, November 2005

Kuyt, G.; Regnier, E. & Gilberti, R. (2006). Optical fiber behavior in radioactive environments, presented at *IEEE ICC meeting*, St-Peterburg, 2006

Lee[a], Bongsoo; Jang, Kyoung Won; Cho, Dong Hyun; Yoo, Wook Jae; Kim, Hyung Shik; Chung, Soon-Cheol & Yi, Jeong Han (2007). Development of one-dimensional fiber-optic radiation sensor for measuring dose distributions of high energy photon beams, *Opt. Rev.*, Vol. 14, No. 5 (2007) (351–354)

Lee[b], Bongsoo; Jang, Kyoung Won; Cho, Kyoung Won; Yoo, Wook Jae; Tack, Gye-Rae; Chung, Soon-Cheol; Kim, Sin & Cho, Hyosung. (2007). Measurements and elimination of Cherenkov light in fiber-optic scintillating detector for electron beam therapy dosimetry, *Nucl. Instr. Methods Phys. Res.* Vol. A579, (2007), (344-348), doi:10.1016/j.nima.2007.04.074

Liu, Y.-P.; Chen, Z.-Y.; Ba, W.-Z.; Fan, Y-W.; Du, Y.-Z.; Pan, S.-L. & Guo, Q. (2008). A study on the real-time radiation dosimetry measurement system based on optically stimulated luminescence, *Chinese Phys. C (HEP & NP)*, Vol. 32, No. 5, (May 2008), (381-384)

Lopez-Higuera, J. M. (1998). *Optical Sensors*, Universidad de Cantabria

Lu, P.; Bao, X.; Kulkarni, N. & Brown, K. (1999). Gamma ray radiation induced visible light absorption in P-doped silica fibers at low dose levels, *Radiat. Meas.*, Vol. 30, (1999), (725-733)

Mady, F.; Benabdesselam, M., Mebrouk, Y. & Dussardier, B. (2010). Radiation effects in ytterbium-doped silica optical fibers: traps and color centers related to the radiation-induced optical losses, *RADECS 2010 Proceedings*, Paper LN2, http://hal.archives-ouvertes.fr/hal-00559422/en/

Magne, S.; De Carlan,L.-L.; Sorel, S.; Bordy, J.-M.; Isambert, A. & Bridier, A. (2008). MAESTRO Project: evelopment of a multi-Channel OSL dosimetricsystemfor clinical use, *Workshop on dosimetric issues in the medical use of ionizing radiation EURADOS AM 2008*, Paris, January 2008

Maier, R. R.J.; MacPherson, W.N.; Barton, J.S.; Jones, J.D.C.; McCulloch, S., Fernandez-Fernandez, A.; Zhang, L. & Chen, X. (2005). Fibre Bragg gratings of type I in SMF-28 and B/Ge fibre and type IIA B/Ge fibre under gamma radiation up to 0.54 MGy,

Proceedeidngs of the 17th International Conference on Optical Fibre Sensors, Voet, M., Willsch, R., Ecke, W., Jones, J. & Culshaw, B. , SPIE Vol. 5855, pp. 511-514, 2005, doi: 10.1117/12.624037

Mao, R.; Zhang, L. & Zhu, R-Y. (2009). Gamma ray induced radiation damage in PWO and LSO/LYSO crystals, *Proceedings of the 2009 IEEE Nuclear Science Symposium Conference Record*, (2009), (2045-2049), http://authors.library.caltech.edu/19580/1/Mao2009p111452008_Ieee_Nuclear_Science_Symposium_And_Medical_Imaging_Conference_(2008_NssMic)_Vols_1-9.pdf

McCarthy, D.; O'Keeffe, S. & Lewis, E. (2010). Optical fibre radiation dosimetry for low dose applications, presented at *IEEE Sensors Conference 2010*, October 2010, Hawaii

McCarthy, D.; O'Keeffe, S.; Sporea, D.; Sporea, A.; Tiseanu, I. & Lewis, E. (2011). Optical Fibre X-Ray Radiation Dosimeter Sensor for Low Dose Applications, presented at *IEEE Sensors Conference 2011*, October 2011, Limerick

McLaughlin, W.L.; Miller, A .; Boyd, A.W.; McDonald, J. C. & Chadwick, K.H. (1989). *Dosimetry for Radiation Processing*, Taylor & Francis, 1989, ISBN-13: 9780850667400

Merlo, J.P & Cankoçak, K. (2006). Radiation-hardness studies of high OH−content quartz fibers irradiated with 24 GeV protons, *CMS Conference Report*, January 2006, http://cdsweb.cern.ch/record/926539/files/CR2006_005.pdf

Miniscalco, W.J.; Wei, T. & Onorato, P.K. (1986). Radiation hardened silica-based optical fibers, *RADC-TR-88-279 - Final Technical Report December 1986*, Rome Air Development Center, Air Force Systems Command, GTE Laboratories

Moloney, W.E. (2008). *A fiber-optic coupled point dosimetry system for the characterization of multi-detector computer tomography*, Master of Science Thesis, University of Florida, 2008

Mommaert, C. (1992). Optoelectronic readout for scintillating fiber trackers, *Nucl. Instr. Met. Phys. Res.*, Vol. A323, (1992), (477-484)

Naka, R.; Watanabe, K.; Kawarabayashi, J.; Uritani, A.; Iguchi, T.; Hayashi, N.; Kojima, N.; Yoshida, T.; Kaneko, J.; Takeuchi, H. & Kakuta, T. (2001). Radiation distribution sensing with normal optical fiber, *IEEE T. Nucl. Scie.*, Vol. 48, No. 6, (December 2001), (2348-2351)

Nakajima, D.; Őzel-Tashenov, B.; Bianchin, S.; Borodina, O.; Bozkurt, V.; Göküzüm, B.; Kavatsyuk, M.; Minami, S.; Rappold, C.; Saito, T.R.; Achenbach, P.; Ajimura, S.; Ayerbe, C.; Fukuda, T.; Hayashi, Y.; Hiraiwa, T.; Hoffmann, J.; Koch, K.; Kurz, N.; Lepyoshkina, O.; Maas, F.; Mizoi, Y.; Mochizuki, T.; Moritsu, M.; Nagae, T.; Nungesser, L.; Okamura, A.; Ott, W.; Pochodzalla, J.; Sakaguchi, A.; Sako, M.; Schmidt, C.J.; Sugimura, H.; Tanida, K.; Träger, M.; Trautmann, W. & Voltz, S. (2009). Scintillating fiber detectors for the HypHI project at GSI, *Nucl. Instr. Met. Phys. Res.*, Vol. A608, (2009), (287–290), doi:10.1016/j.nima.2009.06.068

Nishiura, R. & Izumi, N. (2001). Radiation sensing system using an optical fiber, *Mitsubishi Electric ADVANCE*, September 2001, pp. 25-28

Okamoto, K.; Toh, K.; Nagata, S.; Tsuchiya, B.; Suzuki, T.; Shamoto, N. & Shikama, T. (2004). Temperature dependence of radiation induced optical transmission loss in fused silica core optical fiber, *J. Nucl. Mater.*, Vol. 329–333, (2004), (1503–1506), doi:10.1016/j.jnucmat.2004.04.243

O'Keeffe, S.; Fernandez Fernandez, A.; Fitzpatrick, C.; Brichard, B. & Lewis, E. (2007). Real-time gamma dosimetry using PMMA optical fibres for applications in the sterilization industry, *Meas. Sci. Technol.*, Vol. 18, No. 10, (2007), (3171-3176)

O'Keeffe, S.; Fitzpatrick, C.; Lewis, E. & Al-Shamma'a, A.I. (2008). A review of optical fibre radiation dosimeters, *Sensor Rev.*, Vol. 28, No. 2, (2008), (136–142), doi 10.1108/02602280810856705

O'Keeffe, S. & Lewis, E. (2009). Polymer optical fibre for in situ monitoring of gamma radiation processes, *Intl. J. Smart Sensing and Intelligent Systems,* VOL. 2, No. 3, (September 2009), (490-502)

O'Keeffe[a], S.; Lewis, E.; Santhanam, A. & Rolland, J.P. (2009), Variable Sensitivity Online Optical Fibre Radiation Dosimeter, presented at *The Eighth IEEE Conference on Sensors (IEEE Sensors Conference)*, October 2009, Christchurch

O'Keeffe[b], S.; Lewis E.; Santhanam, A.; Winningham, A. & Rolland, J.P. (2009). Low dose plastic optical fibre radiation dosimeter for clinical dosimetry applications, presented at *The Eighth IEEE Conference on Sensors (IEEE Sensors Conference)*, October 2009, Christchurch

Ong, C.L.; Kandaiya, S.; Kho, H.T. & Chong, M.T. (2009). Segments of a commercial Ge-doped optical fiber as a thermoluminescent dosimeter in radiotherapy, *Radiat. Meas.*, Vol. 44, (2009), (158–162), doi:10.1016/j.radmeas.2009.01.011

Origlio, G. (2009). *Properties and radiation response of optical fibers: role of dopants*, PhD Thesis, http://portale.unipa.it/export/sites/www/dipartimenti/fisica/home/attachments/tesi_dottXXI/Origlio_PhD.pdf

Paul, M.C.; Bohra, D.; Dhar, A.; Sen, R.; Bhatnagar, P.K. & Dasgupta, K. (2009). Radiation response behavior of high phosphorous doped step-index multimode optical fibers under low dose gamma irradiation, *J. Non-Cryst. Solids,* Vol. 355, (2009), (1496-1507), doi:10.1016/j.jnoncrysol.2009.05.017

Pittet, P.; Lua, Guo-Neng; Galvana, J.-M.; Loisya, J.-Y.; Ismaild, A.; Giraudd, J.-Y. & Balossod, J. (2009). Implantable real-time dosimetric probe using GaN as scintillation material, *Sensors Actuators A: Physical*, Vol. 151, (2009), (29–34), doi:10.1016/j.sna.2009.02.018

Plazas, M. C.; Justus, B. L.; Falkenstein, P.; Huston, A. L.; Ning, H. & Miller, R. (2005). Optical fiber detectors as in-vivo dosimetry method of quality assurance in radiation therapy, *Revista Colombiana de Física*, Vol. 37, No. 1, (2005), (307-313)

Primak, W.; Edwards, E.; Keiffer, D. & Szymansk, H. (1964). Ionization expansion of compacted silica and the theory of radiation-induced dilatations in vitreous silica, *Phys. Rev.*, Vol. 133, No. 2A, (January 1964), (A531-A535)

Pruett, B. L.; Peterson, R. T.; Smith, D. E.; Looney, L. D. & Shelton, Jr., R. N. (1984). Gamma-ray to Cerenkov-light conversion efficiency for pure-silica-core optical fibers, *SPIE Proceedings*, Vol. 506, pp. 10-16, San Diego, August 1984

Radiation effects, The 10 th Europhysical Conference on Defects in Insulation Materials, *Phys. Status Solidi*, Vol. 4, No. 3 , (2007), (1060-1175)

Regnier, E.; Flammer, I.; Girard, S.; Gooijer, F.; Achten, F. & Kuyt, G. (2007). Low-dose radiation-induced attenuation at Infrared wavelengths for P-doped, Ge-doped and pure silica-core optical fibres, *IEEE T. Nucl. Sci.*, Vol. 54, No. 4, (August 2007), (1115-1119), doi: 10.1109/TNS.2007.894180,

http://indico.cern.ch/getFile.py/access?contribId=1&resId=1&materialId=0&confId=37455

Rüdiger, F.; Körfer, M.; Göttmann, W.; Schmidt, G. & Wille, K. (2008). Beam loss position monitoring with optical fibres at DELTA, *Proceedings of EPAC 2008*, pp. 1032-1034, Genoa, June 2008

Saint-Gobain Crystals and Detectors (2005). *Scintillating Optical Fibers*, http://www.detectors.saint-gobain.com/uploadedFiles/SGdetectors/Documents/Brochures/Scintillating-Optical-Fibers-Brochure.pdf

Santiago, M.; Prokic, M.; Molina, P.; Marcazzó, J. & Caselli, E. (2009). A tissue-equivalent radioluminescent fiberoptic probe for in-vivo dosimetry based on Mn-doped lithium tetraborate, *WC 2009, IFMBE Proceedings 25/ III*, Dössel, O. & Schlegel, W C. (Eds.), pp. 367–370, 2009

Seo, M.W; Kim, J.K. & Park, J.W. (2009). Gamma-ray induced radiation M. W damage in a small size inorganic scintillator, *The Tenth International Conference on Inorganic Scintillators and their Applications SCINT 2009*, Jeju, June 2009

Seo, M.W; Kim, J.K. & Park, J.W. (2011). Test of a fiber optic scintillation dosimeter with BGO tip in a ^{60}Co irradiation chamber, *Progress in Nucl. Scie. and Techn.*, Vol. 1, (2011), (186-189)

Shikama, T.; Toh, K.; Nagata, S.; Tsuchiya, B.; Yamauchi, M.; Nishitani, T.; Suzuki, T.; Okamoto, K.; Kubo, N.; Ishihara, M. & Kakuta, T. (2004). Optical fast neutron and gamma-ray detection by radioluminescence, *JAERI-Review*, (2004-017), (101-105)

Skuja, L; Tanimura, K & Itoh, N. (1996). Correlation between the radiation-induced intrinsic 4.8 eV optical absorption and 1.9 eV photoluminescence bands in glassy SiO_2, *J. Appl. Phys.*, Vol. 80, No. 6, (Septemer 1996), (3518 – 3525), doi: 10.1063/1.363224

Sporea, D. & Sporea, R. (2005). Setup for the in situ monitoring of the irradiation-induced effects in optical fibers in the ultraviolet-visible optical range, *Rev. Sci. Instrum.*, Vol. 76, No. 11, (2005), doi:10.1063/1.2130932

Sporea, D. & Sporea, A. (2007). Radiation effects in sapphire optical fibers, Phys. Status Solidi (c), Vol. 4, No. 3, (2007), (1356–1359), doi: 10.1002/pssc.200673709

Sporea[a], D., Agnello, S. & Gelardi, F.M. (2010). Irradiation Effects in Optical Fibers, In: *Frontiers in Guided Wave Optics and Optoelectronics*, Pal, B., pp. 49-66, Intech, ISBN 978-953-7619-82-4, Vienna, Austria

Sporea[b], D.; Sporea, A.; Oproiu, C.; Vata, I.; Negut, D.; Secu, M & Grecu, M. (2010). Annual Report, Contract 12084/2008

Suchowerska, N.; Lambert, J.; Nakano, T.; Law, S.; Elsey, J. & McKenzie, D.R. (2007). Afibre optic dosimeter customised for brachytherapy, *Radiat. Meas.*, Vol. 42, (2007), (929–932), doi:10.1016/j.radmeas.2007.02.042

Takada, E.; Kimura, A.; Hosono, Y.; Takahashi, H. & Nakazawa, M. (1999). Radiation distribution sensor with optical fibers for high radiation fields, *J. Nucl. Sci. Techn.*, Vol. 36, No. 8, (August 1999), (641-645)

Tanyi, J. A.; Nitzling, K.D.; Lodwick, C.J.; Huston, A.L. & Justus, B.L. (2011). Characterization of a gated fiber-optic-coupled detector for application in clinical electron beam dosimetry, *Med. Phys.*, Vol. 38, No. 2, (February 2011), (961-967), doi: 10.1118/1.3539737

Thériault, S. (2006). Radiation effects on COTS laser-optimized multimode fibers exposed to an intense gamma radiation field, presented at *Photonics North*, Quebec City, June 2006

Toh, K.; Shikama, T.; Kakuta, T.; Nagata, S.; Tsuchiya, B.; Mori, C.; Hori, J. & Nishitani, T. (2002). Studies of radioluminescence in fused silica core optical fibers, *Proc. SPIE*, Vol. 4786, (2002), doi:10.1117/12.451745

Toh, K.; Shikama, T.; Nagata, S.; Tsuchiya, B.; Suzuki, T.; Okamoto, K.; Shamoto, N.; Yamauchi, M. & Nishitani, T. (2004). Optical characteristics of aluminum coated fused silica core fibers under 14 MeV fusion neutron irradiation, *J. Nucl. Mater.*, Vol. 329–333, (2004), (1495–1498), doi:10.1016/j.jnucmat.2004.04.245

Treadaway, M.J.; Passenheim, B.C. & Kitterer, B.D. (1975). Luminescence and absorption of electron-irradiated common optical glasses, sapphire, and quartz, IEEE *T. Nucl. Sci.*, Vol.22, No. 6, (1975), (2253-2258), doi: 10.1109/TNS.1975.4328115

Tremblay, N.M.; Hubert-Tremblay, V.; Rachel Bujold, Rachel; Beaulieu, L. & Lepage, M. (2010). Improvement in the accuracy of polymer gel dosimeters using scintillating fibers, *J. Phys. Conf. Ser.*, Vol. 250, (2010), (1-4), doi:10.1088/1742-6596/250/1/012076

Tsuchiya, B.; Kondo, S.; Tsurui, T.; Toh, K.; Nagata, S. & Shikama, T. (2011). Correlation between radiation-induced defects, and optical properties of pure fused silica-core optical fiber, under gamma-ray irradiation in air at 1273 K, *J. Nucl. Mater.*, (2011), in press, doi:10.1016/j.jnucmat.2010.12.164

Vedda, A.; Chiodini, N.; Di Martino, D.; Fasoli, M.; Keffer, S.; Lauria, A.; Martini, M.; Moretti, F.; Spinolo, G.; Nikl, M.; Solovieva, N. & Brambilla, G. (2004). Ce3+-doped fibers for remote radiation dosimetry, *Appl. Phys. Lett.*, Vol. 85, No. 26, (December 2004), (6356–6358), doi: 10.1063/1.1840127

Weeks, R. A. & Sonder, E. (1963). The relation between the magnetic susceptibility, electron spin resonance, and the optical absorption of the E1'center in fused silica, In: *Paramagnetic Resonance II*, W. Low, pp. 869-879, Academic Press, LCCN 63-21409, New York

Weinert, A. (1999) *Plastic Optical Fibers*, Publicis MCD Verlag

Wijnands, T.; De Jonge, L.K.; Kuhnhenn, J.; Hoeffgen, S. K. & Weinand, U. (2007). Radiation tolerant optical fibres for LHC beam instrumentation, presented at the *6th LHC Radiation Workshop*, CERN, September 2007

Wittenburg, K. (2008). Beam loss monitors, http://cdsweb.cern.ch/record/1213279/files/p249.pdf

Wrobel, F. (2005). Fundamentals on Radiation-Matter Interaction, *New Challenges for Radiation Tolerance Assessment, RADECS 2005 Short Course Notebook*, Cap d'Agde, September 2005

Wu, F.; Ikram, K. & Albin, S. (2003). Photonic Crystal Fiber for Radiation Sensors, presented at *Workshop on Innovative Fiber Sensors*, Newport News, May 2003

Wulf, F. & Körfer, M. (2009). Beam loss and beam monitoring with optical fibers, *Proceedings of 9th European Workshop on Beam Diagnostics and Instrumentation for Particle Accelerators*, pp. 411-417, Basel, May 2009

Yaakob, N.H.; Wagiran, H.; Hossain, I.; Ramli, A.T.; Bradley, D.A.; Hashim, S.; Ali, H. (2011). Electron irradiation response on Ge and Al-doped SiO_2 optical fibres, *Nucl. Instr. Met. Phys. Res.*, Vol. A637, (2011), (185–189), doi:10.1016/j.nima.2011.02.041

Yoshida, H. & Ichikawa, T. (1995). Temperature effect on the radiation-degradation of poly(methyl methacrylate), *Radiat. Phys. Chem.*, Vol. 46, No. 4-6, Part 1, (1995), (921-924), doi:10.1016/0969-806X(95)00293-7

Yoshida, Y.; Muto, S. & Tanabe, T. (2007). Measurement of soft X-ray excited optical luminescence of a silica glass, In: *CP882, X-ray Absorption Fine Structure – XAFS*73, Hedman, B. & Pianetta, P., 2007, American Institute of Physics

Yukihara, E.G.; Sawakuchi, G.O.; Guduru, S.; McKeever, S.W.S.; Gaza, R.; Benton, E.R.; Yasuda, N.; Uchihori, Y. & Kitamura, H. (2006). Application of the optically stimulated luminescence (OSL) technique in space dosimetry, *Radiat. Meas.*, Vol. 41, (2006), (1126 – 1135), doi:10.1016/j.radmeas.2006.05.027

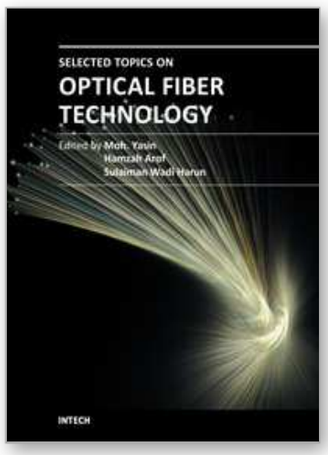

Selected Topics on Optical Fiber Technology

Edited by Dr Moh. Yasin

ISBN 978-953-51-0091-1

Hard cover, 668 pages

Publisher InTech

Published online 22, February, 2012

Published in print edition February, 2012

This book presents a comprehensive account of the recent advances and research in optical fiber technology. It covers a broad spectrum of topics in special areas of optical fiber technology. The book highlights the development of fiber lasers, optical fiber applications in medical, imaging, spectroscopy and measurement, new optical fibers and sensors. This is an essential reference for researchers working in optical fiber researches and for industrial users who need to be aware of current developments in fiber lasers, sensors and other optical fiber applications.

How to reference

In order to correctly reference this scholarly work, feel free to copy and paste the following:

Dan Sporea, Adelina Sporea, Sinead O'Keeffe, Denis McCarthy and Elfed Lewis (2012). Optical Fibers and Optical Fiber Sensors Used in Radiation Monitoring, Selected Topics on Optical Fiber Technology, Dr Moh. Yasin (Ed.), ISBN: 978-953-51-0091-1, InTech, Available from: http://www.intechopen.com/books/selected-topics-on-optical-fiber-technology/optical-fibers-and-optical-fiber-sensors-used-in-radiation-monitoring

INTECH
open science | open minds

InTech Europe
University Campus STeP Ri
Slavka Krautzeka 83/A
51000 Rijeka, Croatia
Phone: +385 (51) 770 447
Fax: +385 (51) 686 166
www.intechopen.com

InTech China
Unit 405, Office Block, Hotel Equatorial Shanghai
No.65, Yan An Road (West), Shanghai, 200040, China
中国上海市延安西路65号上海国际贵都大饭店办公楼405单元
Phone: +86-21-62489820
Fax: +86-21-62489821

IntechOpen